

## Comparative Decellularization and Recellularization of Wild Type and Alpha 1,3 Galactosyltransferase Knockout Pig Lungs: A Model for *Ex Vivo* Xenogeneic Lung Bioengineering and Transplantation

Joseph Platz<sup>a#</sup>, Nicholas R. Bonenfant<sup>a#</sup>, Franziska E. Uhl<sup>a</sup>, Amy L. Coffey<sup>a</sup>, Tristan McKnight<sup>a</sup>, Charles Parsons<sup>a</sup>, Dino Sokocevic<sup>a,1</sup>, Zachary D. Borg<sup>a</sup>, Ying Wai Lam<sup>b</sup>, Bin Deng<sup>b</sup>, Julia G. Fields<sup>b</sup>, Michael DeSarno<sup>c</sup>, Roberto Loi<sup>d</sup>, Andrew M. Hoffman<sup>e</sup>, John Bianchi<sup>g</sup>, Brian Dacken<sup>h</sup>, Thomas Petersen<sup>i</sup>, Darcy E. Wagner<sup>a,j</sup>, Daniel J. Weiss<sup>a,\*</sup>

<sup>a</sup>Department of Medicine, University of Vermont College of Medicine, Burlington VT 05405

<sup>b</sup>Department of Biology and VGN Proteomics Facility, University of Vermont College of Arts and Sciences, Burlington VT 05405

<sup>c</sup>Biostatistics Unit, University of Vermont College of Medicine, Burlington VT 05405

<sup>d</sup>Department of Biomedical Sciences, University of Cagliari, Italy

<sup>e</sup>Department of Clinical Sciences, Tufts University, Cummings School of Veterinary Medicine, 01536

<sup>g</sup>Revivicor, Inc., Blacksburg, VA, 24060

<sup>h</sup>United Therapeutics Corp, Research Triangle Park, North Carolina 27709

<sup>i</sup>Comprehensive Pneumonology Center, Helmholtz Center Munich, Ludwig Maximilians University Munich,

<sup>j</sup>Exemplar Genetics, Exemplar Genetics 958 North Main Sioux Center, Iowa 51250

# Dr. Platz and Mr. Bonenfant are co-1<sup>st</sup> authors

\*Corresponding Author:

Daniel J. Weiss MD Ph.D. (dweiss@uvm.edu)  
Professor of Medicine

Joseph Platz MD (joseph.platz@uvmhealth.org)

Nicholas Bonenfant (nicholas.bonenfant@med.uvm.edu)

Franziska Uhl PhD (franziska.uhl@med.uvm.edu)

Amy Coffey (amy.coffey@uvm.edu)

Tristan McKnight (tmcknight@uvm.edu)

Charles Parsons MD (cparsons@uvm.edu)

Dino Sokocevic (dino.sokocevic@med.uvm.edu)

Zachary Borg (zachary.borg@med.uvm.edu)

<sup>a</sup> University of Vermont College of Medicine  
226 Health Science Research Facility, Burlington, VT 05405  
Phone: 802-656-8925, Fax: 802-656-8926

Ying Wai Lam PhD (Ying-Wai.Lam@uvm.edu)  
Bin Deng PhD (bin.deng@uvm.edu)  
Julia Fields (Julia.fields@uvm.edu)  
<sup>b</sup> 311 Marsh Life Sciences  
Burlington, VT 05405  
Phone: (802) 656-9722, Fax: (802) 656-2914

Michael Desarno PhD (mdesarno@uvm.edu)  
Department of Biostatistics  
<sup>c</sup> University of Vermont College of Medicine  
Burlington, VT 05405

Roberto Loi PhD (rloi@unica.it)  
<sup>d</sup> Department of Biomedical Sciences  
University of Cagliari, Italy  
Phone: 070-675-8638, Fax: 070-666-062

Andrew Hoffman DVM DVSc (Andrew.Hoffman@tufts.edu)  
Department of Clinical Sciences  
Director, Regenerative Medicine Laboratory  
<sup>e</sup> Tufts University, Cummings School of Veterinary Medicine  
Bldg 21, Suite 102, 200 Westboro Road.  
North Grafton, MA 01536

John Bianchi (jbianchi@revivicor.com)  
<sup>g</sup> Revivicor, Inc.  
1700 Kraft Drive Suite 2400  
Blacksburg, VA 24060

Brian Dacken (brian.dacken@exemplargenetics.com)  
<sup>h</sup> Exemplar Genetics  
958 North Main  
Sioux Center, Iowa 51250

Thomas Petersen MD PhD (tpetersen@unither.com)  
Principal Scientist, Regenerative Medicine  
<sup>i</sup> United Therapeutics Corp  
55 T.W. Alexander Drive  
P.O. Box 14186  
Research Triangle Park, North Carolina 27709

Darcy Wagner PhD (Darcy.wagner@helmholtz-muenchen.de).  
<sup>j</sup> Comprehensive Pneumology Center, Helmholtz Center Munich, Ludwig Maximilians University Munich, University Hospital Grosshadern, Member of the German Center for Lung Research (DZL), Munich, Germany

Max-Lebsche-Platz 31 81377 München, Germany  
Conflict of Interest

Thomas Petersen is an employee of United Therapeutics Inc, sponsor of this study.

John Bianchi is an employee of Revivacor, a subsidiary of United Therapeutics, Inc.

Brian Dacken is an employee of Exemplar Genetics, a service provider to Revivacor, Inc.

Daniel Weiss has received funding from United Therapeutics to conduct these studies

Running Title: Xenogeneic pig lung decellularization and recellularization

Keywords: Acellular matrix; alpha 1,3 galactosyltransferase knockout, decellularized lung, extracellular matrix (ECM); lung; pig

## Abstract

**Background:** A novel potential approach for lung transplantation could be to utilize xenogeneic decellularized pig lung scaffolds that are recellularized with human lung cells. However, pig tissues express several immunogenic proteins, notably galactosylated cell surface glycoproteins resulting from alpha 1,3 galactosyltransferase ( $\alpha$ -gal) activity, that could conceivably prevent effective use. Use of lungs from  $\alpha$ -gal knock out ( $\alpha$ -gal KO) pigs presents a potential alternative and thus comparative de- and recellularization of wild type and  $\alpha$ -gal KO pig lungs was assessed.

**Methods:** Decellularized lungs were compared by histologic, immunohistochemical, and mass spectrometric techniques. Recellularization was assessed following compartmental inoculation of human lung bronchial epithelial cells (HBE), human lung fibroblasts (HLF), and human bone marrow-derived mesenchymal stromal cells (MSCS) (all via airway inoculation) and of human pulmonary vascular endothelial cells (CBF) (vascular inoculation).

**Results:** No obvious differences in histologic structure was observed but an approximate 25% difference in retention of residual proteins was determined between decellularized wild type and  $\alpha$ -gal KO pig lungs, including retention of  $\alpha$ -galactosylated epitopes in acellular wild type pig lungs. However, robust initial recellularization and subsequent growth and proliferation was observed for all

cell types with no obvious differences between cells seeded into wild type vs  $\alpha$ -gal KO lungs.

**Conclusion:** These proof of concept studies demonstrate that decellularized wild type and  $\alpha$ -gal KO pig lungs can be comparably decellularized and comparably support initial growth of human lung cells, despite some differences in retained proteins.  $\alpha$ -Gal KO pig lungs are a suitable platform for further studies of xenogeneic lung regeneration.

**Funding:** NIH ARRA RC4HL106625 (DJW), NHLBI R21HL108689 (DJW), the Vermont Lung Center CoBRE grant (P20RR15557), the NIH PACT program (contract HHSN268201000008C), NHBLI Lung Biology Training grant T32 HL076122, NIH Institutional Development Award (IDeA) NIGMS grant P20GM103449, NCRR grant P40RR017447, and United Therapeutics Corporation.

## Introduction

Approximately 1,000-1,500 lung transplants per year are performed in the United States, but a significant shortage of suitable donor lungs and the drawbacks of lung transplantation, including lifelong immunosuppression and an approximate 50% 5-year mortality, demonstrates the critical need for new approaches (1). Use of acellular lung scaffolds for *ex vivo* lung bioengineering has been increasingly investigated as an alternative approach that could potentially allow use of cadaveric or otherwise suboptimal donor lungs following decellularization and seeding with autologous stem or progenitor cells obtained from the eventual transplant recipients (reviewed in 2-4). In particular, recent progress with decellularization and initial recellularization of human lungs has demonstrated the potential feasibility of this approach (5-11). However, not all cadaveric or suboptimal donor lungs may be suitable. In particular, those that originate from aged donors, donors with pre-existing structural lung diseases, or a combination of both age and lung disease may not be suitable. For example, we have recently found that emphysematous changes impair recellularization of both rodent and human lungs and that aging and emphysematous injury further impaired recellularization in rodent models (10,12). Other work has demonstrated that decellularized human lung scaffolds obtained from patients with idiopathic pulmonary fibrosis (IPF) promote a fibrotic phenotype (myofibroblast differentiation) of inoculated fibroblasts (6,13). Therefore, it is unlikely that lungs with any sort of pre-existing lung disease could be used in a clinical translation

scheme. This significantly limits the supply of lungs to be conceivably used in de-cellularization and recellularization approaches.

One potential alternative is to utilize a xenogeneic approach for lung decellularization and recellularization. Ideally the lungs would be procured from a readily available animal source which shares structural and physiologic attributes of human lungs, for which there are no potential ethical or other concerns, and that have minimal antigenic mismatch. To this end, domestic pigs (*Sus scrofa*) may provide a viable option as the size and general anatomy of adult pig lungs are conducive to consideration for use in human transplantation. Use of acellular pig lung scaffolds is thus an appealing option but brings additional challenges with respect to xenogeneic antigens. The alpha (1,3)-galactose ( $\alpha$ -gal) epitope on glycolipids and glycoproteins is the major porcine xenoantigen recognized by xenoantibodies (14,15). This epitope is formed by alpha (1,3)-galactosyltransferase, which is present in all mammals except man, apes, and Old World monkeys (14,15). Both pre-clinical and clinical data demonstrate that following processing of other porcine tissues, such as heart valves and dermal grafts, both native and decellularized tissues may contain residual  $\alpha$ -galactosylated proteins that contribute to immune response and graft failures (16-20). One significant concern therefore is that acellular pig lung scaffolds might also contain residual immunogenic galactosylated proteins. One strategy utilized has been to treat native or acellular grafts with  $\alpha$ -galactosidase to remove any residual  $\alpha$ -galactosylated epitopes (21,22). Another strategy has been to utilize tissues arising from transgenic pigs that lack expression of this enzyme ( $\alpha$ -gal

KO); heart valves and dermal grafts obtained from  $\alpha$ -gal KO pigs are significantly less immunogenic (23). As such, use of acellular lungs from  $\alpha$ -gal KO pigs offers a potentially less immunogenic scaffold for xenogeneic consideration.

We therefore conducted an initial investigation as to whether decellularized  $\alpha$ -gal KO pig lungs recellularized with human cells might present a viable option for consideration in developing strategies for use in clinical bioartificial lung transplantation. Using an optimized detergent-based protocol developed for large (human and pig) lungs, decellularized wild type vs  $\alpha$ -gal KO pig lungs were comparatively assessed using histologic, immunohistochemical, and mass spectrometric analyses (9-11). We then utilized a high throughput approach for seeding alginate-coated decellularized lung segments through physiologically relevant seeding routes (11) and assessed initial growth and subsequent behavior over a four week period between wild type and  $\alpha$ -gal KO pig lungs using four different relevant human cell types: human bronchial epithelial cells (HBE), human lung fibroblasts (HLF), human bone marrow-derived mesenchymal stromal cells (hMSCs), and human pulmonary vascular endothelial cells (CBF).

## Results

*Decellularized wild type and  $\alpha$ -gal KO pig lungs have similar gross histologic appearance and qualitatively retain most major ECM proteins by histologic and immunohistochemical evaluations*

Using an optimized Triton X-100/sodium deoxycholate (SDC) detergent-based decellularization protocol with constant flow perfusion (2 liters/minute) of both the vasculature and airways, wild type and  $\alpha$ -gal KO pig lungs underwent parallel successful decellularization as gauged by progressive loss of pink coloration and a final translucent pearly white appearance (**Figure 1**). The details of the decellularization protocol including rinse volumes are presented in **Supplemental Table 1**.

One important endpoint in whole lung decellularization is the maintenance of major airway and vascular structures and basement membrane composition, while removing cells and clearing cellular material. Following decellularization of both wild type and  $\alpha$ -gal KO pig lungs, we observed similar maintenance of the major histologic and extracellular matrix structures as assessed by hematoxylin and eosin (H&E), Verhoeff's Van Gieson (EVG), Masson's trichrome, and Alcian blue stains, (**Figure 2A**). As previously noted in decellularized rodent, non-human primate, and human lungs, there is qualitative loss of elastin as assessed by the Verhoeff's Van Gieson stain (9-12, 24-26). Similarly, we observed a qualitative loss of lung glycosaminoglycans, many of which are likely cell-associated, as assessed by Alcian blue staining (**Figure 2A**). Transmission electron microscopy demonstrated no obvious difference in ultrastructural

architecture between decellularized wild type and  $\alpha$ -gal KO pig lungs and confirmed maintenance of the alveolar structure, despite the use of pumps and higher flow rates (**Figure 2B**). Minimal residual DNA was observed in decellularized wild type and  $\alpha$ -gal KO pig lungs as assessed qualitatively on DNA gels (**Figure 2C**).

We further evaluated detergent concentration in the effluents during decellularization from 4 wild type and 2  $\alpha$ -gal KO pig lung decellularizations. The wild type data was previously published but displayed at absolute absorbance (27). SDC concentration was reduced in the effluents with each consecutive wash step after incubation in SDC overnight. We found no significant difference in detergent concentrations between the effluents from wild type vs.  $\alpha$ -gal KO pig lungs (**Supplemental Figure 1**).

Immunohistochemical staining for major ECM proteins including types 1 and 4 collagen, fibronectin, and laminin, demonstrated general retention with no obvious qualitative differences between decellularized wild type and  $\alpha$ -gal KO pig lungs (**Figures 3A, B**). Similar to the Verhoeff's Van Gieson stains, immunostaining for elastin was qualitatively decreased and somewhat fragmented appearing in both wild type and  $\alpha$ -gal KO pig lungs. Similar qualitative appearance of residual representative cytoskeletal proteins smooth muscle actin (SMA) and myosin (SMM) was observed in decellularized wild type and  $\alpha$ -gal KO pig lungs (**Figures 3C**).

*Decellularized wild type but not  $\alpha$ -gal KO pig lungs can display evidence of residual galactosylated proteins or debris*

Previously, the  $\alpha$ -gal epitope has been detected in both native and decellularized rodent and porcine tissues (16-20). Histochemical staining for isolectin B4, a standard approach for detecting galactosylated proteins (28), demonstrates diffuse presence of galactose residues in the native wild type but not native  $\alpha$ -gal KO pig lungs (**Figure 4**). As expected, no isolectin B4 staining is observed in decellularized  $\alpha$ -gal KO pig lungs. In general, well-decellularized wild type lungs, as assessed by absence of visible nuclei on H&E stains and by absence of intact DNA on DNA gels, did not have evidence of significant isolectin B4 staining. However, we did observe small sporadic patches of positive isolectin B4 staining, possibly corresponding to residual protein debris or  $\alpha$ -galactosylated matrix proteins (**Figure 4**). Pre-adsorbing the lectin with galactose prior to staining virtually abolished this staining and therefore demonstrates the specificity of this approach (28). This suggests that residual galactosylated proteins or debris exists in acellular wild type pig lungs. As expected, there is no isolectin B4 staining observed in decellularized  $\alpha$ -gal KO pig lungs. These results suggest that incompletely decellularized or even scattered areas of incomplete decellularization in otherwise well-decellularized lungs could result in retention of potentially immunogenic galactosylated proteins or protein debris (**Supplemental Figure 2**).

*Mass spectrometric analyses demonstrate minimal differences between protein content of decellularized wild type vs  $\alpha$ -gal KO pig lungs*

We have previously demonstrated that semi-quantitative mass spectrometric assessment of trypsin-digested acellular lung scaffolds is a powerful means of assessing many residual proteins, including both ECM and a range of cell-associated proteins, following lung decellularization (9-12, 24-26). While not all proteins can be detected using current techniques, in part due to variability in protein solubility and difficulties in detecting low molecular weight proteins, this is an important technique for reliably assessing comparative differences as well as analyzing trends in residual proteins between different acellular scaffolds obtained from different types of lungs or experimental conditions. We thus compared 6 wild type and 10  $\alpha$ -gal KO similarly decellularized pig lungs using this approach where proteins were positively identified with two or more unique peptide hits and were subsequently categorized in one of six groups based on cellular or extracellular location: cytosolic, ECM, cytoskeletal, nuclear, membrane-associated, and secreted (9-12, 24-26). Heatmaps were generated from the log normal transformation of unique peptide hits from each positively identified protein for visual comparison (**Figure 5**). Insets for each protein category show more detail than the general patterns depicted in the combined all proteins heatmap. In general, there was good concordance between individual lungs within the wild type and  $\alpha$ -gal KO groups and a similar general detection of important ECM proteins (collagens, laminins) and cytoskeletal proteins (tubulins, myosins) between the groups (**Supplemental Tables 2 and 3**). However, there

were significant differences in approximately 25% of residual proteins detected in the decellularized wild type vs  $\alpha$ -gal KO lungs. Other statistically significant differences between decellularized wild type and  $\alpha$ -gal KO lungs are summarized in **Supplemental Tables 4 and 5**. Both decellularized wild type and  $\alpha$ -gal KO lungs variably contained differing amounts of residual cytoskeletal, cytosolic, or nuclear proteins detected by mass spectrometry. This highlights previous observations that even lungs considered well decellularized by criteria such as absence of cells, nuclei, and cell debris on histologic evaluations, and absence of significant amounts of residual DNA may still have a range of retained non-ECM proteins (29,30).

*Human lung epithelial cells, lung fibroblasts, and mesenchymal stromal cells demonstrate comparable seeding patterns, histologic appearance, and viability after inoculation into decellularized wild type and  $\alpha$ -gal KO lungs.*

Using a high-throughput technique we have previously developed utilizing alginate-coated small segments (approx. 1 cm<sup>3</sup> segments dissected from the decellularized whole pig lungs (11), we inoculated individual segments with one of four different human cell types including airway epithelial (HBE), vascular endothelial (CBF), lung fibroblasts (HLF), and bone marrow-derived mesenchymal stromal cells (hMSC). Cells were inoculated into physiologically relevant compartments through either small airways (HBE, HLF, hMSC) or blood vessels (CBF) of the small segments. Following inoculation and overnight incubation of the segments at 37°C, each segment was sliced into approximately

1-2 mm thick sections, each of which was cultured individually, submerged in appropriate cell culture medium for up to one month. Initial cell binding and localization as well as growth over the month period were assessed.

One day following airway inoculation of hMSCs, HBEs, or HLFs into either acellular wild type or  $\alpha$ -gal KO scaffolds, HLFs and hMSCs were primarily localized in alveolar spaces and parenchymal regions (**Figures 6A-D, panels A and E**). HBEs were also predominantly observed in parenchymal regions (**Figures 6A-D, panel C**). Notably, HBEs, as with other cell types that did not engraft to the ECM and remained in the airspaces unattached to any matrix, demonstrated rounding up of cells and nuclear fragmentation, consistent with anoikis or apoptosis (24-26). One day after vascular inoculation, the CBFs appeared to be primarily localized in small and medium blood vessels (**Figure 6A-D, panel G**).

Viable HBEs, HLFs, and hMSCs were observed through 28 days of culture (**Figure 6A-D, panel B,D,F**) without any obvious difference in localization or histologic appearance of cells seeded in wild type vs  $\alpha$ -gal KO scaffolds. In contrast, viable CBFs were only robustly observed through 7 days of culture in both wild type or  $\alpha$ -gal KO scaffolds with only sporadic cells occasionally observed at 28 days (**Figure 6A-D, panel H**). At 28 days, HBEs, HLFs, and hMSCs were primarily localized in atelectatic appearing regions of parenchymal lung in both wild type vs  $\alpha$ -gal KO scaffolds although there were scattered areas of cells observed in less atelectatic-appearing areas of alveolar septa. These results are consistent with what we have previously observed following similar

cell seedings in decellularized mouse and human lungs (9-12, 24-26). The atelectatic appearance may reflect production of ECM proteins by the cells themselves, contraction of the matrix by the seeded cells, or collapse due to the natural recoil of lung tissue (26). After 7 days in culture, the CBFs tended to be sparsely localized in blood vessels throughout the lung parenchyma; further, we observed considerably more apoptotic-appearing cells in CBF inoculations than the other three cell types investigated.

Qualitatively assessing proliferation by Ki-67 staining demonstrated scattered positive staining at both day 1 and at day 28 (HBE, HLF, hMSC) or day 7 (CBF) without any obvious difference between cells seeded into wild type vs  $\alpha$ -gal KO scaffolds (**Figure 7A**). Qualitatively assessing early apoptosis by caspase-3 staining demonstrated comparable scattered qualitative caspase-3 staining in HBEs and HLFs in both wild type and  $\alpha$ -gal KO lungs at both day 1 and day 28 (**Figure 7B**). Minimal caspase-3 staining was observed for hMSCs and CBFs seeded into either wild type or  $\alpha$ -gal KO lungs at any time point assessed. Quantitative data analyses of Ki67 and caspase 3 stainings (**Figure 7C**) showed no major differences between hMSC seedings into wild type vs.  $\alpha$ -gal KO lungs on either day 1 or day 28. There was significantly less Ki67 staining and significantly greater caspase-3 staining in CBFs seeded into the  $\alpha$ -gal KO scaffolds compared to the wildtype scaffolds on day 1. However, this difference was not apparent on day 28. There was increased Ki67 staining on day 28 in HLFs seeded into the  $\alpha$ -gal KO scaffolds. In parallel, there was significantly more caspase-3 staining in day 28 vs day 1 HLF seedings in wild type scaffolds with a

near significant increase in the  $\alpha$ -gal KO scaffolds. A similar trend towards increased caspase 3 staining was observed on day 28 seeding of hMSC and CBFs, regardless of scaffold type.

## Discussion

To investigate the potential applicability of decellularized pig lungs for xenogeneic lung transplantation approaches, wild type and  $\alpha$ -gal KO pig lungs were decellularized using an optimized standardized detergent based protocol (9) and compared using qualitative and quantitative histologic, DNA gel and content, immunohistochemical, detergent content, and mass spectrometric techniques we have previously utilized to assess decellularized rodent, non-human primate, and human lungs (9-12, 24-26). Notably, no consistent significant differences were observed between decellularized wild type and  $\alpha$ -gal KO pig lungs in most endpoints. There were some differences in residual protein content in decellularized wild type vs  $\alpha$ -gal KO pig lungs as assessed by mass spectrometry. Ancillary findings included similar propensity of both wild type and  $\alpha$ -gal KO pig lungs to develop blebs during the decellularization scheme as we have previously noted in pig lungs as compared to rodent or human lungs (data not shown, 9). Whether this resulted from over-pressurization during the constant flow decellularization approach utilized remains unclear as does the implication of bleb formation for potential clinical use of acellular pig lung scaffolds. Ancillary findings also included demonstration of residual cytoskeletal, cytosolic, and nuclear proteins in acellular scaffolds produced from both wild type and  $\alpha$ -gal KO pig lungs. These findings are expected based on our previous, consistent observations of retention of  $\alpha$ -smooth muscle actin and smooth muscles myosin in decellularized rodent, pig, non-human primate, and human lungs (9,10,12,24-26). An important finding of this study is that residual galactosylated proteins

and/or debris may be present in wild type porcine lungs judged to be otherwise well-decellularized by other outcome measures. This suggests that a number of potentially immunogenic cellular proteins can remain in decellularized lungs and promotes consideration of  $\alpha$ -gal KO pig lungs for use in xenogeneic lung transplantation approaches. However, as in comparable studies in decellularized rodent and human lungs, this did not appear to affect cell inoculation and behavior in wild type vs  $\alpha$ -gal KO pig lungs. We observed similar initial recellularization and subsequent growth and qualitative appearances over one month for two different types of differentiated lung cells and one additional stromal cell population seeded into decellularized wild type vs  $\alpha$ -gal KO pig lungs. In contrast, human pulmonary vascular endothelial cells only survived robustly for a relatively brief period in both wild type and  $\alpha$ -gal KO pig lungs. As further discussed below, there are several potential reasons for the relatively poor survival of the endothelial cells, however, the critical issue for this level of comparison is that they behaved similarly in the  $\alpha$ -gal KO as in the wild type pig lungs. There were some significant differences observed in Ki67 and caspase-3 staining between CBFs seeded into wild type vs  $\alpha$ -gal KO pig lungs at day 1. These might reflect real differences between the lungs or these differences might be attributed to the small sample size and will need to be further explored in a larger study.

Recent progress in approaches for producing and studying decellularized lungs has promoted rapid advances in the field (2-4). Using an optimized detergent-based approach we have recently developed for large animal and

human lungs, and using a combination of histologic, immunohistochemical, and mass spectrometric techniques, we and others have found that comparable to decellularization of rodent and human lungs, anatomic structure and the content of major ECM proteins is preserved in decellularized pig lungs (5,7,8,9). However, the presence of residual galactosylated proteins and/or debris in lungs judged to be otherwise well-decellularized by other outcome measures suggests that more aggressive decellularization approaches or post-decellularization treatment with  $\alpha$ -galactosidases might be necessary to remove the immunogenic  $\alpha$ -galactosylated epitopes (21,22,31,32). Several groups have developed automated decellularization protocols for porcine and human lungs, including large volume rinses between the decellularization steps (5,7,8). These presumably will be more effective at removing residual proteins and debris, but more aggressive decellularization processes might remove components necessary for recellularization, such as growth factors sequestered to the matrix, as well as damaging or degrading the ECM scaffold (33). Future analyses need to be performed to assess for the immunogenic alpha-gal epitope and other potentially immunogenic residual proteins in decellularized pig lungs.

Using physiologic inoculation of epithelial, stromal, and endothelial cells into acellular wild type and  $\alpha$ -gal KO pig lungs, we did not observe any differences in initial seeding or in subsequent growth of the inoculated cells over a one month period, with the exception of CBF cells which only lasted in significant numbers until the seven day time point in both wild type and  $\alpha$ -gal KO acellular pig lungs. Initial proliferation and early apoptosis was different in CBFs

seeded into wild type vs  $\alpha$ -gal KO pig lungs although these differences weren't apparent at 28 days. This suggests that despite differences in residual proteins detected using the mass spectrometry technique utilized here, an admittedly incomplete assessment of the full range of residual proteins, these proteins don't seem to make a difference in recellularization using the cells and approaches utilized for these studies, by histologic assessment. To fully understand the implications of the range of residual proteins and glycoproteins found in decellularized lungs, further investigation like quantification by western blot and other methods, and functional assessments will help clarify the role of the remaining proteins. This is particularly important given the qualitative information provided by techniques such as immunohistochemical assessment of selected residual proteins. In particular, despite a number of recent studies assessing residual proteins in decellularized lungs, their functional role either positively in supporting cell growth and differentiation or negatively in potentially serving as immunogenic foci, remains unclear.

The relatively poor survival of the vascular endothelial cells may reflect several factors including lack of vascular perfusion and also perhaps a non-permissive environment for the particular cells utilized. Further studies with more primitive endothelial progenitor precursors may provide more robust growth. In parallel, recent advances in perfusion and ventilation approaches for supporting cell growth and function following seeding of acellular lungs, will allow further support of long term cell growth (34,35).

However, there remain many questions for utilizing acellular pig lung scaffolds, particularly those derived from  $\alpha$ -gal KO pigs. Our preliminary data investigating seeding with differentiated lung and stromal cells will be followed up with comparable studies using other cell populations including but not limited to induced pluripotent stem (iPS) cells and different populations of endogenous lung progenitors. Further study of environmental variables such as mode of perfusion and ventilation is also necessary to optimize recellularization and production of functional lung tissue.

Further, as continued progress is being made in techniques for whole lung de- and recellularization, fundamental questions remain about the potential immunogenicity of the scaffolds, particularly xenogeneic scaffolds. A tenet of the potential use of recellularized lungs is that they will be non-immunogenic or at least only minimally immunogenic, particularly if recellularized with cells obtained from the eventual transplant recipient. This will reflect both the relative lack of immunogenicity of the decellularized extracellular matrix scaffold and also any potential remodeling by cells seeded into the scaffold that would then mask any potential remaining immunogenic epitopes (36). As the lung is a more structurally complicated organ than heart valves or skin grafts, it may be more difficult to achieve adequate removal of immunogenic proteins. We are currently assessing potential immunogenicity of both wild type and  $\alpha$ -gal KO pig lung scaffolds in a range of *in vitro* and *in vivo* assays.

## Conclusions

Decellularized  $\alpha$ -gal KO pig lung scaffolds can be de- and recellularized similar to results observed in wild type pig lungs. These initial studies provide a firm basis for further investigation into the potential use of  $\alpha$ -gal KO pig lung scaffolds for development of xenogeneic transplant approaches.

## Methods

### *Pig lungs*

Heart-lung blocs were obtained from euthanized wild type pigs (14-18 weeks, male *sus scrofa*) through an IACUC-approved organ sharing program at the University of Vermont. Pigs were induced with ketamine and atropine, maintained on isoflurane and then given an IV dose of sodium pentobarbital (Fatal Plus, Vortech Pharmaceuticals, Dearborn, MI, USA). Lungs from 15  $\alpha$ -gal KO pigs (6-16 weeks) and 8 older pigs (6 months-4 years) were obtained from Revivacor Inc. (Blacksburg, VA, USA) following euthanasia according to AAALAC approved protocols. Lungs from the younger  $\alpha$ -gal KO pig lungs were utilized for decellularization analyses including histologic and mass spectrometric. Five of the  $\alpha$ -gal KO pig lungs were incompletely decellularized and thus not utilized for reseeded studies. Well decellularized lungs from both younger and older pigs were utilized for cell seedings. After euthanasia, the trachea-lung bloc was removed by dissection, the vasculature flushed with sterile saline, packed in ice, and shipped by overnight express. A total of up to 33 wild type and 23  $\alpha$ -gal KO pig lungs were evaluated for the different components of this study.

### *Lung decellularization*

Pig lungs were decellularized under sterile conditions, using a combined perfusion and physical approach we have recently developed after scaling up and optimizing methods initially developed for rodent and small non-human primate models for use in larger pig and human lungs (9-12, 24-26). As

previously demonstrated, a constant perfusion rate of 2 L/minute yielded optimal results for preserving remaining ECM architecture and protein content while minimizing residual cell debris in decellularized human and porcine lungs content (9). For each of the below steps, solutions were infused or perfused at a rate of 2 L/minute using a roller perfusion pump (Stockert Shiley, SOMA Technologies, Bloomfield, CT, USA). On day 1 of the decellularization protocol, the lungs were rinsed six times with 2-3 L for each rinse of de-ionized (DI) water containing 500 IU/mL Penicillin/500 µg/mL Streptomycin (5X pen/strep) (Lonza) through both the trachea and the pulmonary artery. To account for differences in lung or lobe sizes between animals, particularly for larger lungs obtained from older animals, complete filling without overinflating the lungs was used to determine the individual wash volume, resulting in slight variations between lungs. Next, the lungs were rinsed once with Triton solution (4-6 L of 0.1% Triton X-100 (Sigma) and 5X pen/strep in DI water) infused through both the airways and vasculature. Lungs were filled a second time with Triton solution via both airways and vasculature, submerged in Triton solution and incubated for 24 hours at 4°C on a rocker-shaker (Gene Mate, Bio Express, Kaysville, UT, USA). On day 2, the lungs were removed from the Triton solution and rinsed six times with 2-3 L per rinse of DI water and 5X pen/strep. The lungs were then rinsed once with SDC solution (4-6 L of 2% sodium deoxycholate (SDC, Sigma in DI water) and SDC solution was then instilled as previously described for day 1. Lungs were incubated in SDC solution for 24 hours at 4°C on the rocker-shaker. The next day, lungs were removed from the SDC solution and rinsed six times with 2-3L

per rinse of DI water and 5X pen/strep. The lungs were then rinsed once with sodium chloride (NaCl) solution (4-6 L of 1 M sodium chloride (NaCl) (USB) and 5X pen/strep in DI water), filled a second time with the NaCl solution and incubated in the NaCl solution for 1 hour at room temperature (25°C) on the rocker-shaker. Lungs were removed from the NaCl solution, rinsed six times with 2-3L per rinse of DI water and 5X pen/strep as described above. The lungs were then rinsed once with DNase solution (4-6 L of 30 µg/mL porcine pancreatic DNase (Sigma), 2 mM calcium chloride (CaCl<sub>2</sub>) (Sigma), 1.3 mM magnesium sulfate (MgSO<sub>4</sub>) (Sigma), and 5X pen/strep in DI water) filled a second time with DNase solution and incubated for 1 hour at room temperature on the rocker-shaker. The lungs were removed from the DNase solution, rinsed six times with 2-3L per rinse of DI water and 5X pen/strep as described above, then rinsed once with peracetic acid (PAA) solution (4-6 L of 0.1% (v/v) peracetic acid (Sigma) in 4% (v/v) ethanol solution in DI water), instilled a second time with the PAA solution, and incubated for 1 hour at room temperature on the rocker-shaker. Finally, lungs were removed from the PAA solution and rinsed six times with 2-3L per rinse of DI water and 5X pen/strep as described above. After six washes with 2-3 L of storage solution (in total 12-18 L of a 5X pen/strep, 50 mg/L gentamicin (Cellgro), 2.5 µg/mL Amphotericin B (Cellgro) in 1X PBS solution (storage solution) as described for the pen/strep DI water rinses, lungs were stored in storage solution at 4°C until needed, but a maximum for 3 months prior to use. The protocol steps are summarized in **Supplemental Table 1**.

### *Assessment of residual DNA*

Native and decellularized lung tissue was dried on tissue paper (Kimwipe, Kimtech, Kimberly-Clark, Roswell, GA, USA) until no liquid was visibly seen to be released from it, weighed, and DNA was extracted using the DNeasy Blood & Tissue Kit (Qiagen, Hilden, Germany) following the instructions provided by the manufacturer. For qualitative assessment of DNA degradation and size, the same volume of sample per isolated DNA was run on a 0.8% agarose gel and visualized under UV light with SYBR Safe DNA Gel stain (Invitrogen). A 100 bp ladder and salmon sperm DNA (Invitrogen) was used as DNA size marker and positive control.

### *Anionic Detergent Assessment*

Concentrations of SDC in wash effluents were determined using our recently published methylene blue (MB) assay (27). In short: effluent samples were mixed with 0.0125% MB (Sigma-Aldrich) in DI water (w/v) at a ratio of 1:10. After vortexing of the samples with MB, chloroform (Sigma-Aldrich) was added at a ratio of 1:2 (sample: chloroform, v/v). Samples were then vortexed for 1 min. Following a 30 minute incubation period at room temperature, 150  $\mu$ l of the bottom chloroform layer was extracted and the absorbance at 630 nanometers (nm) was measured in a Synergy HT Multi-Detection Microplate Reader (Biotek Instruments, Winooski, VT, USA) in a polypropylene 96-well plate (Costar, Corning, NY, USA). Pure DI-water or PBS (Mediatech Inc., Manassas, VA, USA) containing no detergents served as the blank. SDC concentration was calculated

based on SDC standard curves prepared in either DI water (for Triton, SDC, NaCl, and DNase effluents) or storage solution (for PBS effluents).

### *Lung Histology*

Decellularized lungs were fixed (20 cm H<sub>2</sub>O) with 4% paraformaldehyde for 3 hrs at room temperature, embedded in paraffin, and 5- $\mu$ m sections mounted on glass slides. Following deparaffinization, sections were stained with hematoxylin & eosin, Verhoeff's Van Gieson (EVG), Masson's Trichrome, or Alcian Blue, and were assessed by standard light microscopy (9-12, 24-26).

### *Lectin staining*

Lung tissue samples were deparaffinized with three 15-minute washes in xylene, followed by two 5-minute washes in 100% ethanol, two 5-minute washes in 95% ethanol, one 5-minute wash in 70% ethanol, one 5-minute wash in 50% ethanol, one 5-minute wash in deionized water, and one 5-minute wash in 1% BSA (Sigma #A9647) in PBS. Slides were incubated for 60 minutes with Isolectin GS-IB4 Alexa 568 (Life Technologies #I21412) antibody diluted with 1% BSA at a concentration of 20 $\mu$ g/ml. Some samples were pre-absorbed with galactose during this step, in which case the isolectin antibody preparation was combined with 100 mM galactose (Fisher #S25334) prior to adding to the slides (28). Following incubation at room temperature, samples were washed five times for 5 minutes in 1% BSA. The samples were exposed to DAPI (1:500) (Invitrogen #D1306) in 1% BSA for 15 minutes. These were washed three times for 5

minutes in 1% BSA, and a coverslip was applied using Aqua Polymount (Polysciences #18606) (28).

### *Electron microscopy*

For electron microscopic analyses, segments of decellularized porcine lung were fixed overnight at 4°C in Karnovsky's fixative (2.5% glutaraldehyde, 1.0% paraformaldehyde in 0.1M Cacodylate buffer, pH 7.2). After rinsing in Cacodylate buffer, the tissue was minced into 1mm<sup>3</sup> pieces and then fixed in 1% osmium tetroxide for 2 hours at 4°C. Subsequently, the pieces were rinsed again in Cacodylate buffer, dehydrated through graded ethanols, and then cleared in propylene oxide and embedded in Spurr's epoxy resin (all reagents from Electron Microscopy Sciences, Hatfield PA). Semithin sections (1µm) were cut with glass knives on a Reichert ultracut microtome (Reichert-Jung, Vienna Austria), stained with methylene blue–azure II and then evaluated for areas of interest (proximal and distal alveolar septae, large/small airways, blood vessels). Ultrathin sections (60-80nm) were cut with a diamond knife, retrieved onto 200 mesh thin bar nickel grids, contrasted with uranyl acetate (2% in 50% ethanol) and lead citrate, and examined with a JEOL 1400 TEM (JEOL USA, Inc, Peabody, Ma) operating at 60kV (9).

### *Immunohistochemical (IHC) staining*

Standard deparaffinization was performed with three separate 10 min incubations in xylenes, followed by rehydration in a descending series of ethanols, and finally

in water. Antigen retrieval was performed by heating tissue in 1x sodium citrate buffer (Dako, Carpinteria, CA) at 98°C for 20 minutes followed by a brief 20 minutes cool at room temperature. Tissue sections were permeabilized in 0.1% Triton X-100 solution (Sigma Aldrich, St. Louis, MO) for 15 minutes. Triton X-100 was removed with two 10 minute washes in 1% BSA solution. Blocking was performed with 10% goat serum (Jackson Immuno Research) for 60 minutes. After blocking, primary antibody was added and tissue sections were incubated overnight at 4°C in a humidified chamber. Tissues were washed three times with 1% BSA (Sigma) solution for 5 minutes each. Secondary antibody was added and incubated for 60 min at room temperature in a dark humidified chamber. Tissues were again washed three times in 1% BSA solution for 5 minutes each in the dark. DAPI nuclear stain (Invitrogen/Life Technologies/Thermo Fisher was added for 5 minutes at room temperature in the dark followed by 2 washes in 1% BSA solution for 5 minutes each. The sections were finally mounted in Aqua Polymount (Lerner Laboratories, Pittsburg, PA). Primary antibodies used were: purified mouse anti-fibronectin monoclonal (610077 – 1:100 – BD Transduction Laboratories, Franklin Lakes, NJ, USA), laminin antibody polyclonal (ab11575 – 1:100 – Abcam, Cambridge, United Kingdom), rabbit polyclonal to alpha elastin (ab21607 – 1:100 – Abcam), smooth muscle myosin heavy chain 2 polyclonal (ab53219 – 1:100 – Abcam), collagen I polyclonal (ab292 – 1:100 – Abcam), Ki67 proliferation marker polyclonal (ab16667 - 1:50 - Abcam), cleaved caspase-3 polyclonal (Asp175 – 1:100 – Cell Signaling Technology, Danvers, MA, USA), mouse clone anti-human actin polyclonal (1A4 - 1:10,000 - Dako via FAHC,

Denmark). Secondary antibodies used: Alexa Fluor 568 goat anti-rabbit IgG (H+L) (1:500, Invitrogen), Alexa Fluor 568 F(ab')<sub>2</sub> fragment of goat anti-mouse IgG (H+L) (1:500, Invitrogen) (9-11).

For quantitative analyses of Ki67 and caspase-3 stainings, slides from 3 wild type and 3  $\alpha$ -gal KO lungs seeded with each individual cell type were analyzed by Image J (<http://imagej.nih.gov/ij/index.html>). For each seeding and time point, 4 regions/slide were quantified to determine the percentage of positively stained Ki67 or caspase-3 expressing cells (red staining = Ki67/caspase-3, blue staining = DAPI).

### *Mass spectrometry*

Samples of the same approximate weight and volume, (approximately 125 mg and 1 cm<sup>3</sup>, respectively for each sample), were obtained from similar distal parenchymal regions of lungs. Each sample was dried separately in a SpeedVac and suspended in 40  $\mu$ l of 100 mM ammonium bicarbonate (NH<sub>4</sub>HCO<sub>3</sub>) and 50 mM dithiothreitol (DTT) and stored at 56° C for 1 hour. After cooling, 5  $\mu$ l of 500 mM iodoacetamide in 100 mM NH<sub>4</sub>HCO<sub>3</sub> were added and the solution was incubated for 30 min at room temperature in the dark, and then dried in a SpeedVac. The dried tissue was suspended in 50  $\mu$ l of trypsin solution (10 ng/ $\mu$ l) in 50 mM NH<sub>4</sub>HCO<sub>3</sub> and incubated overnight at 37°C. Next, 5  $\mu$ l of 10% formic acid were added to stop the digestion. The sample was centrifuged at 14,000 X g for 10 minutes. 15  $\mu$ l of supernatant were drawn and desalted using a ZipTip C<sub>18</sub> (P10, Millipore Corporation, Billerica, MA) according to the manufacturer's

protocol, and then dried in a SpeedVac. The dried peptide samples were dissolved in 20  $\mu$ l 0.1% formic acid and 2% acetonitrile, and 6  $\mu$ l were loaded onto a fused silica microcapillary LC column (12 cm x 100  $\mu$ m inner diameter) packed with C18 reversed-phase chromatographic materials (5  $\mu$ m particle size; 20 nm pore size; Magic C<sub>18</sub>AQ, Michrom Bioresources Inc.). Peptides were separated by applying a gradient of 3-60% acetonitrile in 0.1% formic acid for 45 min at a flow rate of 500 nL/min. Nanospray ionization was used to introduce peptides into a linear ion trap (LTQ)-Orbitrap mass spectrometer (Thermo Fisher Scientific) via a nanospray ionization source. Mass spectrometry data was acquired in a data-dependent acquisition mode, in which an Orbitrap survey scan from m/z 400-2000 (resolution: 30,000 FWHM at m/z 400) was paralleled by 10 LTQ MS/MS scans of the most abundant ions (37). After an LC-MS run was completed and spectra were obtained, the spectra were searched against the pig protein sequence database compiled from UniProtKB/Swiss Prot database (<http://www.uniprot.org>) in forward and reverse orientations through SEQUEST using Proteome Discoverer software (version 1.4.1.14; Thermo Electron, San Jose, CA). The search parameters permitted a mass tolerance of 2 Da and 1 Da for precursor ions (MS1 scans) and fragment ions (MS/MS scans), respectively. Oxidation of methionine (M) and carbamidomethylation of cysteines (C) were allowed as variable modifications. Up to two missed tryptic cleavages of peptides were considered. All search results (msf files) were imported into Scaffold (version Scaffold\_4.0.5, Proteome Software Inc., Portland, OR) for the calculations of total spectral counts (Normalized Total Spectral Counts option

was used) (37). Parent mass tolerance of 100 ppm, Protein Threshold of 99% and Min # of Peptides = 2 were applied to limit the false discovery rates (FDR) to 0% at peptide level in the data set. Proteins that contained identical peptides and could not be differentiated due to the absence of unique peptides were grouped to satisfy the principles of parsimony. Proteins presented are broadly categorized and ranked by the average number of peptides identified from the replicate samples.

Proteins positively identified with two or more unique peptide hits were assigned to one of six groups: ECM, cytosolic, cytoskeletal, nuclear, membrane-associated, and secreted. Heatmaps were generated with the log normal transformation of unique peptide hits from each positively identified protein (9,10,12). If any of the proteins were matched to more than one category, its predominant subcellular location was chosen for functional grouping. Positive protein identification was assigned based on two or more unique peptide hits within each individual sample, not across all samples.

#### *Preparation and culture of recellularized segments of decellularized lungs*

Small, approximately 2cm<sup>3</sup> pieces of decellularized wild type and  $\alpha$ -gal KO lungs were excised from the larger lobes and blood vessels and/or airways were cannulated with 25g cannula. After the cannulae were secured with titanium clips (Teleflex Medical) the lung segments were coated in 2.5% sodium alginate (Manugel, FMC Biopolymer, Philadelphia, PA, USA) and then immediately cross-linked with a 3% calcium chloride (Sigma) solution, resulting in segments being

uniformly coated in a calcium alginate hydrogel (11). Hydrogel-coated segments were then inoculated with cell suspensions ( $1-5 \times 10^6$  cells per segment) and allowed to incubate at 37°C overnight. Segments were then sliced into approximately 1mm sections with sterile razor blades and each slice placed in a well of a 24-well non-tissue culture treated dish, covered with 2mL of sterile cell cultivation media, and placed in a standard tissue culture incubator at 37°C with 5% CO<sub>2</sub> as previously described (11). Slices were harvested at 1, 3, 7, 14, 21, and 28 days post-inoculation and fixed for 1 hr at room temperature in 4% paraformaldehyde. Harvested samples were embedded in paraffin, cut and mounted as 5µm sections, and then assessed by H&E staining for the presence and distribution of the inoculated cells.

#### *Cells and cell inoculation*

Human bronchial epithelial cells (HBE) (courtesy of Albert van der Vliet, University of Vermont, originally from Drs. J. Yankaskas and R. Wu (38) were cultured on cell-culture treated plastic at 37°C and 5% CO<sub>2</sub> in serum free culture medium consisting of DMEM/F-12 50/50 mix (Corning), 10 ng/ml Cholera toxin (Sigma), 10 ng/ml epidermal growth factor (Sigma), 5 µg/ml insulin (Gemini Bio-Products, West Sacramento, CA, USA), 5 µg/ml transferrin (Sigma), 0.1 µM dexamethasone (Sigma), 15 µg/ml bovine pituitary extract (Sigma), 0.5 mg/ml bovine serum albumin (Life Technologies), and 100 IU/ml penicillin/100 µg/ml streptomycin (Corning). Human Lung Fibroblasts (HLF) (ATCC, CCL 171) and are grown in media consisting of DMEM/F-12 50/50 mix (Corning), 10% fetal

bovine serum (Hyclone), 100 IU/ml penicillin/100 µg/ml streptomycin (Corning), 2mM L-glutamine (Corning). CBF (pulmonary endothelial colony forming cells) cells were obtained from Mervin Yoder (Indiana University – Purdue University Indianapolis) and grown in cEGM-2 (Lonza) supplemented with 10% fetal bovine serum (Hyclone, Thermo Scientific), and 100 IU/ml penicillin/100 µg/ml streptomycin (Corning). These cells were expanded on collagen type I coated tissue culture surfaces. Human bone marrow-derived mesenchymal stromal cells (hMSCs) were obtained from the Texas A&M Stem Cell Core facility. These cells have previously been extensively characterized for cell-surface marker expression and differentiation capacity (439). Cells were expanded in culture using media consisting of Modification of Eagle Medium-Earls Balanced Salt Solution (MEM-EBSS) (Hyclone, Thermo Scientific), 20% fetal bovine serum (Hyclone), 100 IU/ml penicillin/100 µg/ml streptomycin (Corning), 2mM L-glutamine (Corning), and used only at passages 7 or 8.

### *Statistical Analyses*

For mass spectrometry assessments, heat maps for the natural log of unique peptide hits for each positively identified protein in the mass spectrometric analyses of lungs de-cellularized under each experimental condition were generated using the 'pheatmap' package for 'R' statistical software version 2.15.1. Comparisons of median unique peptide count between the two groups (alpha-gal vs wild type) were done using the non-parametric exact permutation test, with  $p < 0.05$  considered statistically significant (37). This non-parametric

equivalent of the t-test was used due to the non-normality of the data and the small sample sizes per group. As a measure of agreement/concordance of mass spectrometry proteomic proteins between lungs, non-parametric Spearman correlations were also done, with concordance considered significant at  $p < 0.05$  (37). The exact permutation tests and correlations were done using SAS statistical software, version 9.2. Differences between Ki67 or caspase-3 expression were assessed by two way ANOVA with Bonferroni post-test.

**Author Contributions**

JP: Research study design and implementation, data collection and analyses

NRB: Research study design and implementation, data collection and analyses, manuscript writing

FEU: Data collection and analyses

ALC: Data collection and analyses

TM: Data collection and analyses

CP: Data collection and analyses

DS: Data collection and analyses

ZDB: Data collection and analyses

YWL: Data collection and analyses

BDe: Data collection and analyses

JGF: Data collection and analyses

MD: Data analyses (statistical)

RL: Data collection and analyses

AMH: Research study design and implementation

JB: Provided reagents (transgenic pig lungs)

BDa: Provided reagents (transgenic pig lungs)

TP: Research study design and implementation

DEW: Research study design and implementation, data collection and analyses, manuscript writing

DJW: Project coordinator, research study design and implementation, data collection and analyses, manuscript writing

## Acknowledgements

The authors are grateful to Douglas Taatjes PhD and Nicole Bishop of the UVM Microscopy and Imaging Center for assistance with immunohistochemical and lectin staining and interpretations, and to Jason Friedman, Ethan Griswold, Justin Hawk, Robert J Hommel, Juan Jose Uriarte, and Sean Wrenn for assistance with lung decellularizations.

## References

1. Orens, J.B. and Garrity, E.R. General overview of lung transplantation and review of organ allocation. *Proc Am Thorac Soc* **6**, 13-9, 2009.
2. Prakash, Y.S., Tschumperlin, D.J., and Stenmark, K.R. Coming to terms with tissue engineering and regenerative medicine in the lung. *Am J Physiol Lung Cell Mol Physiol* **309**, L625-38, 2015.
3. Calle, E.A., Ghaedi, M., Sundaram, S., Sivarapatna, A., Tseng, M.K., and Niklason, L.E. Strategies for whole lung tissue engineering. *IEEE Trans Biomed Eng* **61**, 1482-96, 2014.
4. Wagner, D.E., Bonvillain, R.W., Jensen, T., Girard, E.D., Bunnell, B.A., Finck, C.M., Hoffman, A.M., and Weiss, D.J. Can stem cells be used to generate new lungs? Ex vivo lung bioengineering with decellularized whole lung scaffolds. *Respirology* **18**, 895-911, 2013.
5. Gilpin, S.E., Guyette, J.P., Gonzalez, G., Ren, X., Asara, J.M., Mathisen, D.J., Vacanti, J.P., and Ott, H.C. Perfusion decellularization of human and porcine lungs: bringing the matrix to clinical scale. *J Heart Lung Transplant* **33**, 298-308, 2014.
6. Booth, A.J., Hadley, R., Cornett, A.M., Dreffs, A.A., Matthes, S.A., Tsui, J.L., Weiss, K., Horowitz, J.C., Fiore, V.F., Barker, T.H., Moore, B.B., Martinez, F.J., Niklason, L.E., and White, E.S. Acellular normal and fibrotic

- human lung matrices as a culture system for in vitro investigation. *Am J Respir Crit Care Med* **186**, 866-76, 2012.
7. Nichols, J.E., Niles, J.A., and Cortiella, J. Production and utilization of acellular lung scaffolds in tissue engineering. *J Cell Biochem* **113**, 2185-92, 2012.
  8. O'Neill, J.D., Anfang, R., Anandappa, A., Costa, J., Javidfar, J., Wobma, H.M., Singh, G., Freytes, D.O., Bacchetta, M.D., Sonett, J.R., and Vunjak-Novakovic, G. Decellularization of human and porcine lung tissues for pulmonary tissue engineering. *Ann Thorac Surg* **96**, 1046-55; discussion 1055-6, 2013.
  9. Wagner, D.E., Bonenfant, N.R., Sokocevic, D., DeSarno, M.J., Borg, Z.D., Parsons, C.S., Brooks, E.M., Platz, J.J., Khalpey, Z.I., Hoganson, D.M., Deng, B., Lam, Y.W., Oldinski, R.A., Ashikaga, T., and Weiss, D.J. Three-dimensional scaffolds of acellular human and porcine lungs for high throughput studies of lung disease and regeneration. *Biomaterials* **35**, 2664-79, 2014.
  10. Wagner, D.E., Bonenfant, N.R., Parsons, C.S., Sokocevic, D., Brooks, E.M., Borg, Z.D., Lathrop, M.J., Wallis, J.D., Daly, A.B., Lam, Y.W., Deng, B., DeSarno, M.J., Ashikaga, T., Loi, R., and Weiss, D.J. Comparative decellularization and recellularization of normal versus emphysematous human lungs. *Biomaterials* **35**, 3281-97, 2014.

11. Wagner, D., Fenn, S., Bonenfant, N., Marks, E., Borg, Z., Saunders, P., Oldinski, R., and Weiss, D. Design and Synthesis of an Artificial Pulmonary Pleura for High Throughput Studies in Acellular Human Lungs. *Cellular and Molecular Bioengineering* **7**, 184-195, 2014.
12. Sokocevic, D., Bonenfant, N.R., Wagner, D.E., Borg, Z.D., Lathrop, M.J., Lam, Y.W., Deng, B., Desarno, M.J., Ashikaga, T., Loi, R., Hoffman, A.M., and Weiss, D.J. The effect of age and emphysematous and fibrotic injury on the re-cellularization of de-cellularized lungs. *Biomaterials* **34**, 3256-69, 2013.
13. Parker, M.W., Rossi, D., Peterson, M., Smith, K., Sikstrom, K., White, E.S., Connett, J.E., Henke, C.A., Larsson, O., and Bitterman, P.B. Fibrotic extracellular matrix activates a profibrotic positive feedback loop. *J Clin Invest* **124**, 1622-35, 2014.
14. Galili, U. Discovery of the natural anti-Gal antibody and its past and future relevance to medicine. *Xenotransplantation* **20**, 138-47, 2013.
15. Galili, U. Avoiding detrimental human immune response against Mammalian extracellular matrix implants. *Tissue Eng Part B Rev* **21**, 231-41, 2015.
16. Chiang, T.R., Fanget, L., Gregory, R., Tang, Y., Ardiet, D.L., Gao, L., Meschter, C., Kozikowski, A.P., Buelow, R., and Vuist, W.M. Anti-Gal

- antibodies in humans and 1, 3alpha-galactosyltransferase knock-out mice. *Transplantation* **69**, 2593-600, 2000.
17. Lee, C., Ahn, H., Kim, S.H., Choi, S.Y., and Kim, Y.J. Immune response to bovine pericardium implanted into alpha1,3-galactosyltransferase knockout mice: feasibility as an animal model for testing efficacy of anticalcification treatments of xenografts. *Eur J Cardiothorac Surg* **42**, 164-72, 2012.
18. Park, C.S., Oh, S.S., Kim, Y.E., Choi, S.Y., Lim, H.G., Ahn, H., and Kim, Y.J. Anti-alpha-Gal antibody response following xenogeneic heart valve implantation in adults. *J Heart Valve Dis* **22**, 222-9, 2013.
19. Dalmaso, A.P., Vercellotti, G.M., Fischel, R.J., Bolman, R.M., Bach, F.H., and Platt, J.L. Mechanism of complement activation in the hyperacute rejection of porcine organs transplanted into primate recipients. *Am J Pathol* **140**, 1157-66, 1992.
20. Kasimir, M.T., Rieder, E., Seebacher, G., Wolner, E., Weigel, G., and Simon, P. Presence and elimination of the xenoantigen gal (alpha1, 3) gal in tissue-engineered heart valves. *Tissue Eng* **11**, 1274-80, 2005.
21. Choi, S.Y., Jeong, H.J., Lim, H.G., Park, S.S., Kim, S.H., and Kim, Y.J. Elimination of alpha-gal xenoreactive epitope: alpha-galactosidase treatment of porcine heart valves. *J Heart Valve Dis* **21**, 387-97, 2012.

22. Xu, H., Wan, H., Zuo, W., Sun, W., Owens, R.T., Harper, J.R., Ayares, D.L., and McQuillan, D.J. A porcine-derived acellular dermal scaffold that supports soft tissue regeneration: removal of terminal galactose-alpha-(1,3)-galactose and retention of matrix structure. *Tissue Eng Part A* **15**, 1807-19, 2009.
23. Mohiuddin, M.M., Singh, A.K., Corcoran, P.C., Hoyt, R.F., Thomas, M.L., 3rd, Ayares, D., and Horvath, K.A. Genetically engineered pigs and target-specific immunomodulation provide significant graft survival and hope for clinical cardiac xenotransplantation. *J Thorac Cardiovasc Surg* **148**, 1106-13; discussion 1113-4, 2014.
24. Wallis, J.M., Borg, Z.D., Daly, A.B., Deng, B., Ballif, B.A., Allen, G.B., Jaworski, D.M., and Weiss, D.J. Comparative assessment of detergent-based protocols for mouse lung de-cellularization and re-cellularization. *Tissue Eng Part C Methods* **18**, 420-32, 2012.
25. Bonvillain, R.W., Danchuk, S., Sullivan, D.E., Betancourt, A.M., Semon, J.A., Eagle, M.E., Mayeux, J.P., Gregory, A.N., Wang, G., Townley, I.K., Borg, Z.D., Weiss, D.J., and Bunnell, B.A. A nonhuman primate model of lung regeneration: detergent-mediated decellularization and initial in vitro recellularization with mesenchymal stem cells. *Tissue Eng Part A* **18**, 2437-52, 2012.
26. Daly, A.B., Wallis, J.M., Borg, Z.D., Bonvillain, R.W., Deng, B., Ballif, B.A., Jaworski, D.M., Allen, G.B., and Weiss, D.J. Initial binding and

- recellularization of decellularized mouse lung scaffolds with bone marrow-derived mesenchymal stromal cells. *Tissue Eng Part A* **18**, 1-16, 2012.
27. Zvarova, B., Uhl, F.E., Uriarte, J.J., Borg, Z.D., Coffey, A.L., Bonenfant, N.R., Weiss, D.J., and Wagner, D.E. Residual Detergent Detection Method for Nondestructive Cytocompatibility Evaluation of Decellularized Whole Lung Scaffolds. *Tissue Eng Part C Methods* **22**, 418-28, 2016.
28. Taatjes, D.J., Barcomb, L.A., Leslie, K.O., and Low, R.B. Lectin binding patterns to terminal sugars of rat lung alveolar epithelial cells. *J Histochem Cytochem* **38**, 233-44, 1990.
29. Crapo, P.M., Gilbert, T.W., and Badylak, S.F. An overview of tissue and whole organ decellularization processes. *Biomaterials* **32**, 3233-43, 2011.
30. Li, Q., Uygun, B.E., Geerts, S., Ozer, S., Scalf, M., Gilpin, S.E., Ott, H.C., Yarmush, M.L., Smith, L.M., Welham, N.V., and Frey, B.L. Proteomic analysis of naturally-sourced biological scaffolds. *Biomaterials* **75**, 37-46, 2016.
31. Lim, H.G., Choi, S.Y., Yoon, E.J., Kim, S.H., and Kim, Y.J. In vivo efficacy of alpha-galactosidase as possible promise for prolonged durability of bioprosthetic heart valve using alpha1,3-galactosyltransferase knockout mouse. *Tissue Eng Part A* **19**, 2339-48, 2013.
32. Kim, M.S., Jeong, S., Lim, H.G., and Kim, Y.J. Differences in xenoreactive immune response and patterns of calcification of porcine and bovine

- tissues in alpha-Gal knock-out and wild-type mouse implantation models. *Eur J Cardiothorac Surg* **48**, 392-9, 2015.
33. Shojaie, S., Ermini, L., Ackerley, C., Wang, J., Chin, S., Yeganeh, B., Bilodeau, M., Sambhi, M., Rogers, I., Rossant, J., Bear, Christine E., and Post, M. Acellular Lung Scaffolds Direct Differentiation of Endoderm to Functional Airway Epithelial Cells: Requirement of Matrix-Bound HS Proteoglycans. *Stem Cell Reports* **4**, 419-430, 2015.
34. Ren, X., Moser, P.T., Gilpin, S.E., Okamoto, T., Wu, T., Tapias, L.F., Mercier, F.E., Xiong, L., Ghawi, R., Scadden, D.T., Mathisen, D.J., and Ott, H.C. Engineering pulmonary vasculature in decellularized rat and human lungs. *Nat Biotechnol* **33**, 1097-102, 2015.
35. Charest, J.M., Okamoto, T., Kitano, K., Yasuda, A., Gilpin, S.E., Mathisen, D.J., and Ott, H.C. Design and validation of a clinical-scale bioreactor for long-term isolated lung culture. *Biomaterials* **52**, 79-87, 2015.
36. Keane, T.J. and Badylak, S.F. The host response to allogeneic and xenogeneic biological scaffold materials. *J Tissue Eng Regen Med* **9**, 504-11, 2015.
37. Nesvizhskii, A.I., Keller, A., Kolker, E., and Aebersold, R. A statistical model for identifying proteins by tandem mass spectrometry. *Anal Chem* **75**, 4646-58, 2003.

38. Yankaskas, J.R., Haizlip, J.E., Conrad, M., Koval, D., Lazarowski, E., Paradiso, A.M., Rinehart, C.A., Jr., Sarkadi, B., Schlegel, R., and Boucher, R.C. Papilloma virus immortalized tracheal epithelial cells retain a well-differentiated phenotype. *Am J Physiol* **264**, C1219-30, 1993.
39. Sekiya, I., Larson, B.L., Smith, J.R., Pochampally, R., Cui, J.G., and Prockop, D.J. Expansion of human adult stem cells from bone marrow stroma: conditions that maximize the yields of early progenitors and evaluate their quality. *Stem Cells* **20**, 530-41, 2002.

## Figure Legends

**Figure 1: Wild type and  $\alpha$ -gal KO pig lungs are comparably grossly decellularized.** Progressive decellularization results in comparable clearing of blood and pink coloration resulting in final pearly white translucent tissues. Representative images from wild type (n=33) and  $\alpha$ -gal KO (n=17) pig lungs are shown. SDC = sodium deoxycholate, PAA = peracetic acid.

**Figure 2: The decellularization process largely preserves the native structure of porcine lungs.** Representative images of native and decellularized wild type and  $\alpha$ -gal KO pig lungs are depicted. **A)** Photomicrographs demonstrate qualitative preservation of characteristic structure and major ECM proteins (collagen, elastin) by H&E, EVG, and trichrome stains. Glycosaminoglycan content is qualitatively decreased as assessed by Alcian blue staining. Original magnification 100X. a = airways, bv = blood vessels. Representative images from wild type (n=33) and  $\alpha$ -gal KO (n=17) pig lungs are shown. **B)** Transmission electron microscopy demonstrates comparable appearance of proximal airway, distal airway, and alveolar septal regions in decellularized wild type and  $\alpha$ -gal KO pig lungs (scale bar is indicated on each image). Representative images from a single decellularized wild type and single  $\alpha$ -gal KO lung are shown. Enlargements of the inserts for each image demonstrate more detail in residual collagen and elastin fibers (arrows). **C)** DNA gels demonstrate minimal residual DNA in decellularized wild type and  $\alpha$ -gal KO pig lungs compared to native controls. A DNA ladder and salmon sperm DNA (positive control) are shown for

comparison. Representative gels for native and decellularized wild type and  $\alpha$ -gal KO pig lungs are shown.

**Figure 3: Decellularization similarly preserves major ECM proteins in wild type and  $\alpha$ -gal KO pig lungs.** Representative photomicrographs comparing native and decellularized wildtype and  $\alpha$ -gal KO pig lungs are depicted and demonstrate similar qualitative retention of ECM proteins (**A,B**) and smooth muscle myosin and actin. (**C**) Nuclear DAPI staining is depicted in blue and the stain(s) of interest are depicted in red or green. Col1 = type I collagen, Col4 = type 4 collagen, Elast = elastin, Fib = fibronectin, Lam = laminin, SMA = smooth muscle actin, SMM = smooth muscle myosin, bv = blood vessel, a = airway. Original magnifications 100X. a= airways, bv = blood vessels. Representative images from 2 wild type and 11  $\alpha$ -gal KO pig lungs are shown.

**Figure 4: Isolectin B4 staining demonstrates the potential for residual  $\alpha$ -galactosylated proteins or protein debris remaining in decellularized wild type vs  $\alpha$ -gal KO pig lungs.** Small areas of positive (red) staining (arrow, insert) can be sporadically observed in what appear to be otherwise well-decellularized wild type pig lungs as judged by histologic appearance and residual DNA content. In contrast, no lectin staining is observed in either native or decellularized  $\alpha$ -gal KO pig lungs. Original magnification 200X. Representative images from 23 wild type and 18  $\alpha$ -gal KO pig lungs are shown.

**Figure 5: Mass spectrometric assessment of residual proteins following decellularization of wild type vs  $\alpha$ -gal KO pig lungs demonstrates overall concordance in residual proteins detected. A)** Positively identified proteins in decellularized wild type vs  $\alpha$ -gal KO pig lungs (i.e. those proteins which exceeded the FDR cutoff for identification) from each method of decellularization were assigned to groups according to subcellular location (cytoskeletal, cytosolic, ECM, membrane-associated, nuclear, and secreted). Heatmaps were generated using the log normal transformation of total spectral counts for all positively identified proteins and grouped by category. Representative heatmaps from 6 wild type and 10  $\alpha$ -gal KO pig lungs are shown

**Figure 6: HBE, hMSC, and HLFs demonstrate comparable seeding patterns and viability for up to 28 days following inoculation into both wild type and  $\alpha$ -gal KO pig lungs, but CBF cells only survive for 7 days.** Representative H&E low power (100X) photomicrographs show characteristic recellularization patterns one day post-inoculation of each cell type (left column) and the last day viable cells were observed (right column) in acellular wild type (**A,B**) or  $\alpha$ -gal KO (**C,D**) pig lungs. Representative images from 33 wild type and 17  $\alpha$ -gal KO lungs seeded with each cell type are shown. **B,D**) High power (400X) images of the respective seedings into either acellular wild type (B) or  $\alpha$ -gal KO (D) pig lungs. In general, cells that do not interact with the ECM scaffold and remain in the airspaces or vascular spaces unattached to any matrix demonstrated rounding up of cells and nuclear fragmentation, consistent with anoikis or apoptosis.

**Figure 7: Cells seeded into wild type vs  $\alpha$ -gal KO pig lungs demonstrate similar patterns of Ki67 and caspase-3 staining.** **A, B)** Representative photomicrographs one day post-inoculation of each cell type and the last day viable cells were observed are depicted. Original magnification 100X. Ki67 or caspase-3 staining is indicated in red and DAPI nuclear staining in blue. Representative images from 3 wild type and 3  $\alpha$ -gal KO lungs seeded with each cell type are depicted. **C)** Quantitative analysis of randomized images from 3 wild type and 3  $\alpha$ -gal KO lungs seeded with each individual cell type. 4 regions/slide from each seeding and time point were quantified to determine the percentage of ratio of positive stained Ki67 or caspase-3 expressing cells (red staining = Ki67/caspase-3) to total cells (blue staining = DAPI).

**Supplemental Figure 1: Detection of residual anionic detergents in wash effluents during decellularization demonstrated no differences between wild type and  $\alpha$ -gal KO pig lungs.** Depicted is SDC concentration in consecutive DI water washes after incubation of the lungs with the respective decellularization solution. The data from the wild type lungs was already published before as absolute absorption at 630 nm (27) but converted to SDC % concentration and utilized as comparison for the  $\alpha$ -gal KO pig lung effluents.

**Supplemental Figure 2: Isolectin B4 staining in incompletely decellularized wild type pig lungs demonstrates residual  $\alpha$ -galactosylated proteins or protein debris.** Representative image from an incompletely decellularized wild

type pig lung demonstrates areas of positive (red) staining (arrow, insert) can be observed in both non-adsorbed and galactose-preadsorbed lectin stainings along with residual DAPI-positive (blue) cell nuclei. Original magnification 200X.

## Figure Legends

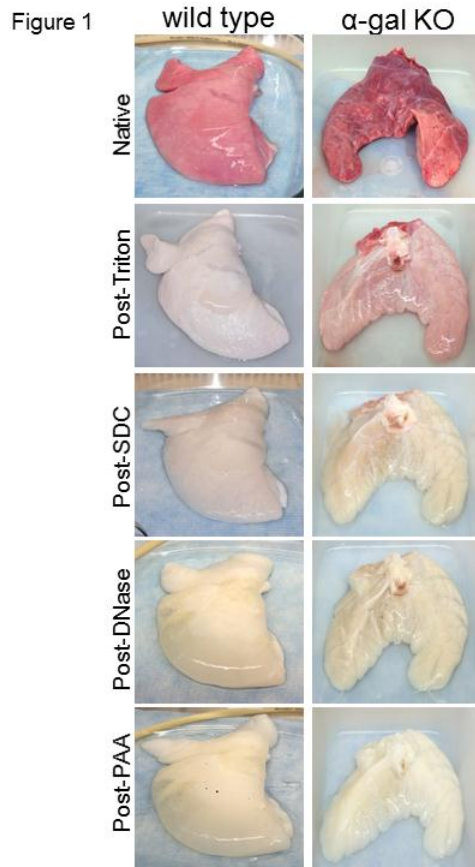
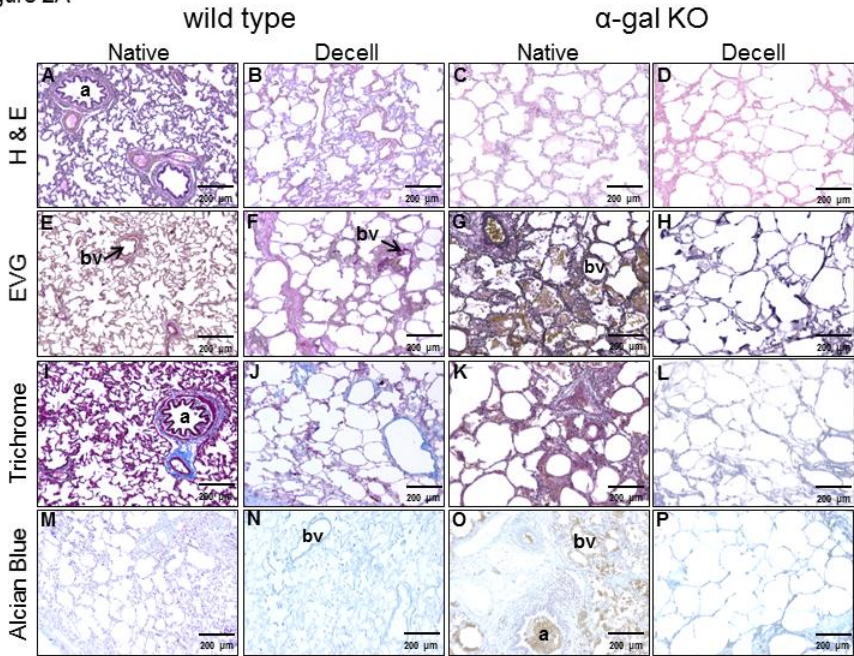


**Figure 1: Wild type and  $\alpha$ -gal KO pig lungs are comparably grossly decellularized.** Progressive decellularization results in comparable clearing of blood and pink coloration resulting in final pearly white translucent tissues. Representative images from wild type (n=33) and  $\alpha$ -gal KO (n=17) pig lungs are shown. SDC = sodium deoxycholate, PAA = peracetic acid.

Figure 2A



Tissue Engineering Part C: Methods  
Comparative study to the use of decellularized alpha-Gal KO pig lungs for xenogeneic lung transplantation (doi: 10.1089/ten.TEC.2016.0109)  
This article has been peer-reviewed and accepted for publication, but has yet to undergo copyediting and proof correction. The final published version may differ from this proof.

Figure 2B

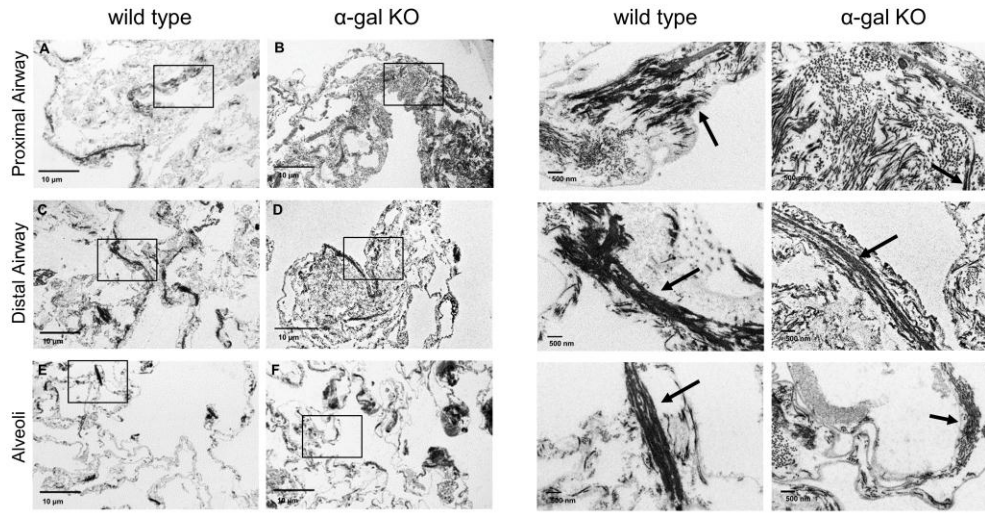
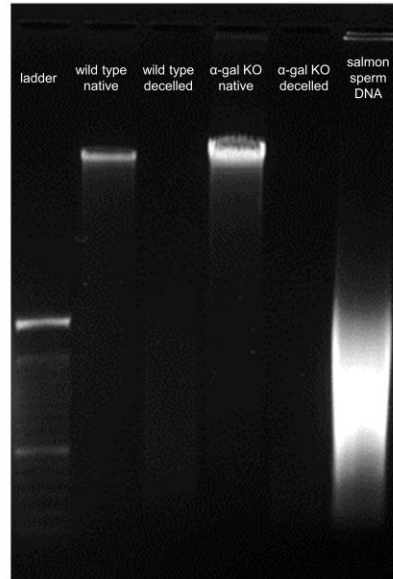


Figure 2C



**Figure 2: The decellularization process largely preserves the native structure of porcine lungs.** Representative images of native and decellularized wild type and  $\alpha$ -gal KO pig lungs are depicted. **A)** Photomicrographs demonstrate qualitative preservation of characteristic structure and major ECM proteins (collagen, elastin) by H&E, EVG, and trichrome stains. Glycosaminoglycan content is qualitatively decreased as assessed by Alcian blue staining. Original magnification 100X. a = airways, bv = blood vessels. Representative images from wild type (n=33) and  $\alpha$ -gal KO (n=17) pig lungs are shown. **B)** Transmission electron microscopy demonstrates comparable appearance of proximal airway, distal airway, and alveolar septal regions in decellularized wild type and  $\alpha$ -gal KO pig lungs (scale bar is indicated on each image). Representative images from a single decellularized wild type and single  $\alpha$ -gal KO lung are shown. Enlargements of the inserts for each image demonstrate more detail in residual collagen and elastin fibers (arrows). **C)** DNA gels demonstrate minimal residual

DNA in decellularized wild type and  $\alpha$ -gal KO pig lungs compared to native controls. A DNA ladder and salmon sperm DNA (positive control) are shown for comparison. Representative gels for native and decellularized wild type and  $\alpha$ -gal KO pig lungs are shown.

Figure 3A

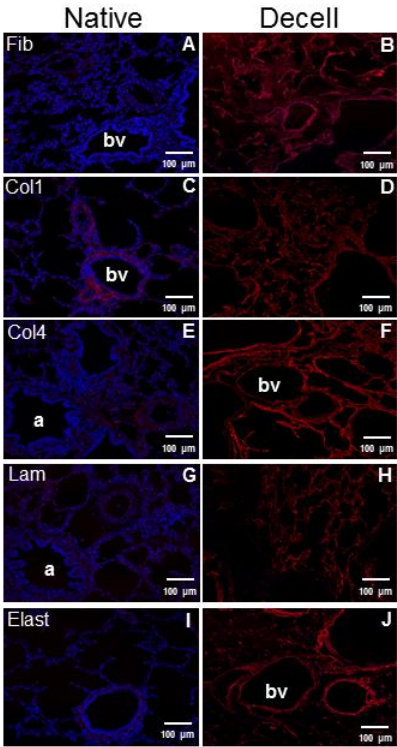


Figure 3B

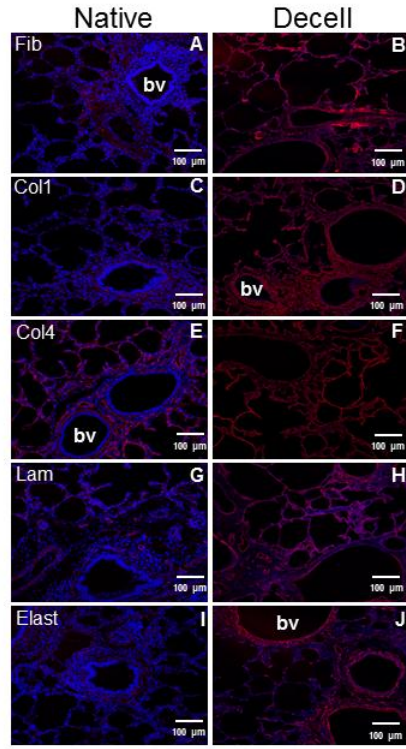
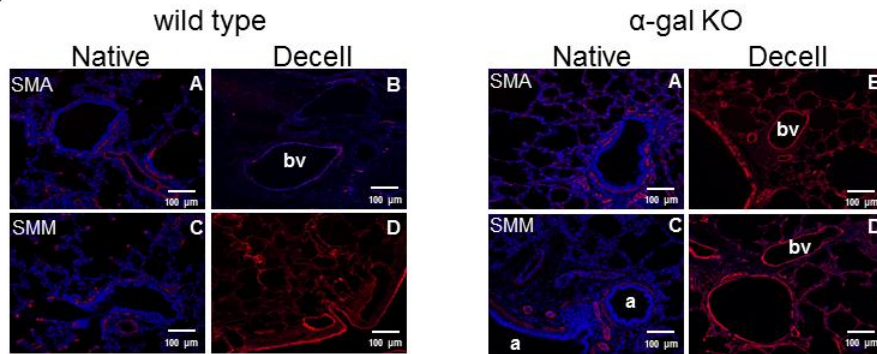


Figure 3C

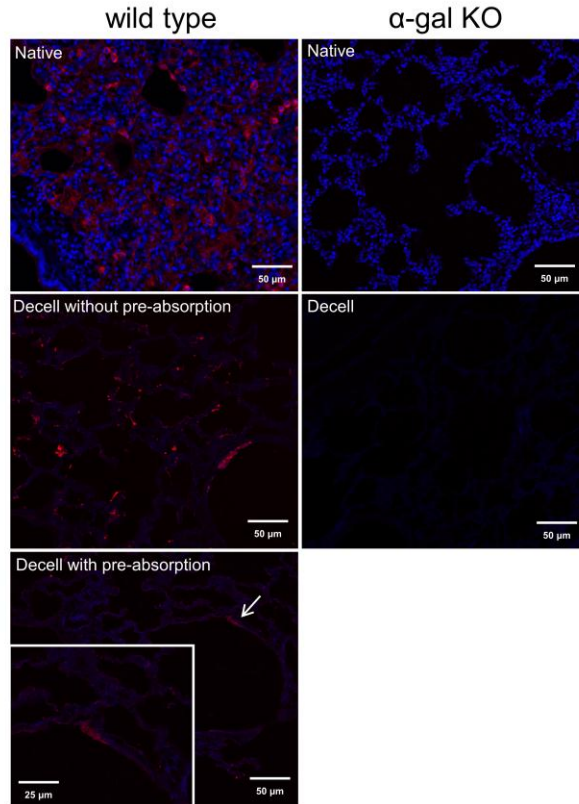


**Figure 3: Decellularization similarly preserves major ECM proteins in wild type and  $\alpha$ -gal KO pig lungs.** Representative photomicrographs comparing native and decellularized wildtype and  $\alpha$ -gal KO pig lungs are depicted and demonstrate similar qualitative retention of ECM proteins (**A,B**) and smooth muscle myosin and actin. (**C**) Nuclear DAPI staining is depicted in blue and the stain(s) of interest are depicted in red or green. Col1 = type I collagen, Col4 = type 4 collagen, Elast = elastin, Fib = fibronectin, Lam = laminin, SMA = smooth muscle actin, SMM = smooth muscle myosin, bv = blood vessel, a = airway. Original magnifications 100X. a= airways, bv = blood vessels. Representative images from 2 wild type and 11  $\alpha$ -gal KO pig lungs are shown.

Comparative study to the use of decellularized alpha-Gal KO pig lungs for xenogeneic lung transplantation (doi: 10.1089/ten.TEC.2016.0109)  
This article has been peer-reviewed and accepted for publication, but has yet to undergo copyediting and proof correction. The final published version may differ from this proof.

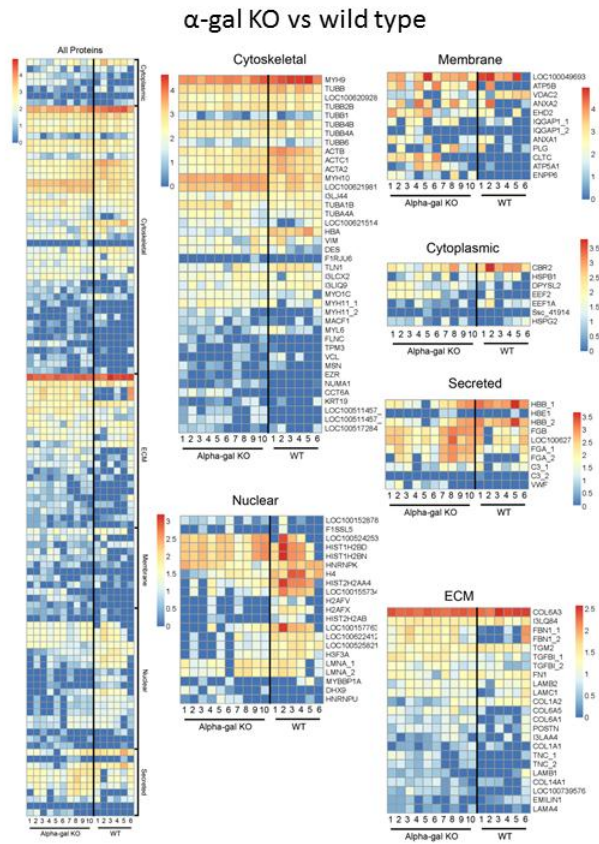
Tissue Engineering Part C: Methods

Figure 4



**Figure 4: Isolectin B4 staining demonstrates the potential for residual  $\alpha$ -galactosylated proteins or protein debris remaining in decellularized wild type vs  $\alpha$ -gal KO pig lungs.** Small areas of positive (red) staining (arrow, insert) can be sporadically observed in what appear to be otherwise well-decellularized wild type pig lungs as judged by histologic appearance and residual DNA content. In contrast, no lectin staining is observed in either native or decellularized  $\alpha$ -gal KO pig lungs. Original magnification 200X. Representative images from 23 wild type and 18  $\alpha$ -gal KO pig lungs are shown.

Figure 5

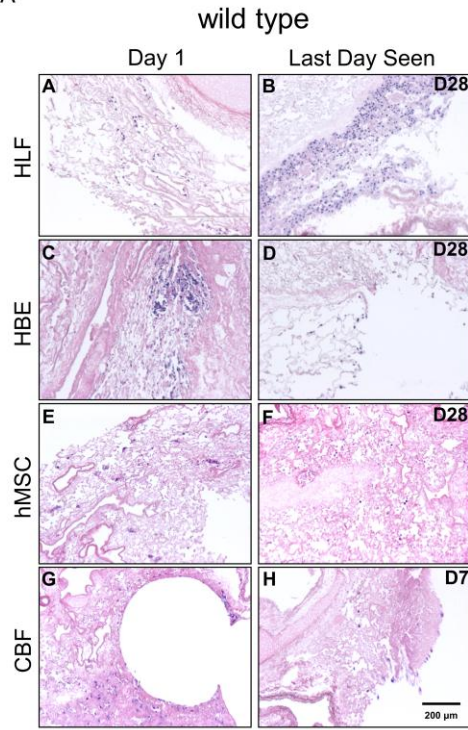


**Figure 5: Mass spectrometric assessment of residual proteins following decellularization of wild type vs  $\alpha$ -gal KO pig lungs demonstrates overall concordance in residual proteins detected. A)** Positively identified proteins in decellularized wild type vs  $\alpha$ -gal KO pig lungs (i.e. those proteins which exceeded the FDR cutoff for identification) from each method of decellularization were assigned to groups according to subcellular location (cytoskeletal, cytosolic, ECM, membrane-associated, nuclear, and secreted). Heatmaps were generated using the log normal transformation of total spectral counts for all positively identified proteins and grouped by category. Representative heatmaps from 6 wild type and 10  $\alpha$ -gal KO pig lungs are shown

Comparative study to the use of decellularized alpha-Gal KO pig lungs for xenogeneic lung transplantation (doi: 10.1089/ten.TEC.2016.0109)  
This article has been peer-reviewed and accepted for publication, but has yet to undergo copyediting and proof correction. The final published version may differ from this proof.

Tissue Engineering Part C: Methods

Figure 6A



Tissue Engineering Part C: Methods  
Comparative study to the use of decellularized alpha-Gal KO pig lungs for xenogeneic lung transplantation (doi: 10.1089/ten.TEC.2016.0109)  
This article has been peer-reviewed and accepted for publication, but has yet to undergo copyediting and proof correction. The final published version may differ from this proof.

Figure 6B

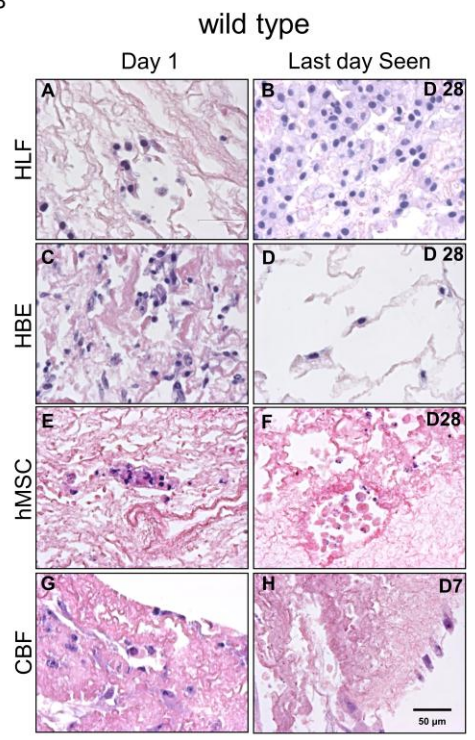


Figure 6C

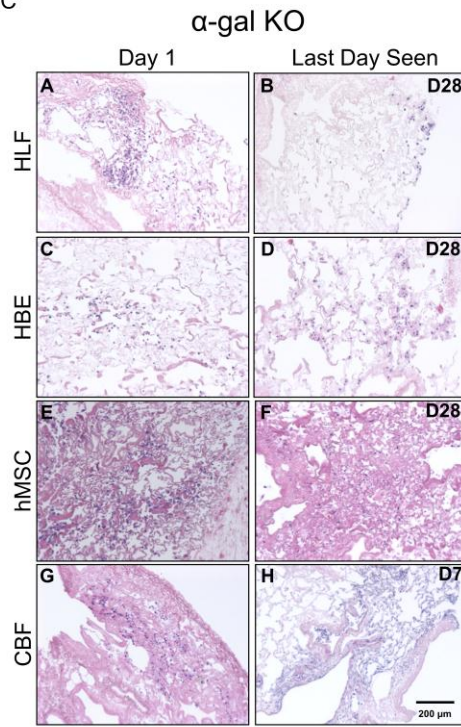
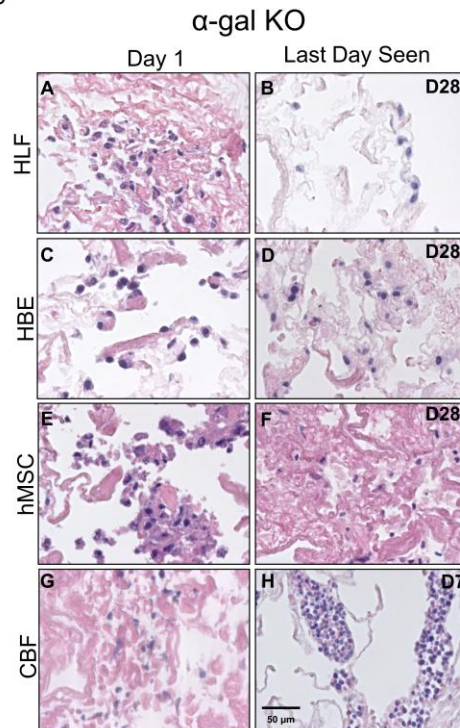


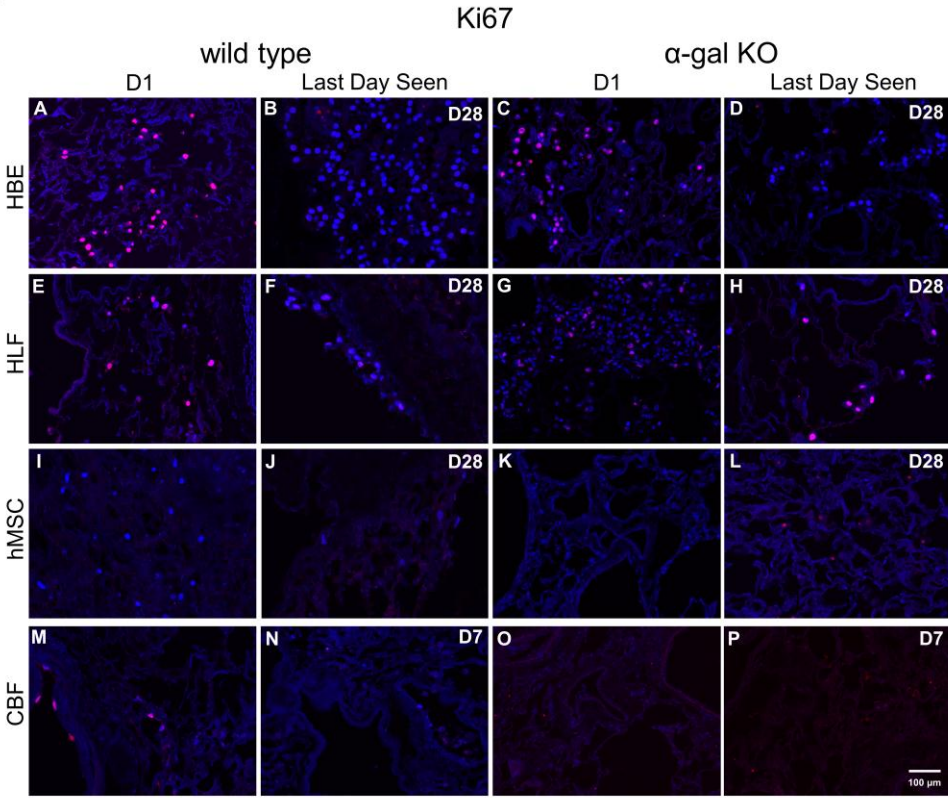
Figure 6D



**Figure 6: HBE, hMSC, and HLFs demonstrate comparable seeding patterns and viability for up to 28 days following inoculation into both wild type and  $\alpha$ -gal KO pig lungs, but CBF cells only survive for 7 days.** Representative H&E low power (100X) photomicrographs show characteristic recellularization patterns one day post-inoculation of each cell type (left column) and the last day viable cells were observed (right column) in acellular wild type (**A,B**) or  $\alpha$ -gal KO (**C,D**) pig lungs. Representative images from 33 wild type and 17  $\alpha$ -gal KO lungs seeded with each cell type are shown. **B,D**) High power (400X) images of the respective seedings into either acellular wild type (B) or  $\alpha$ -gal KO (D) pig lungs. In general, cells that do not interact with the ECM scaffold and remain in the

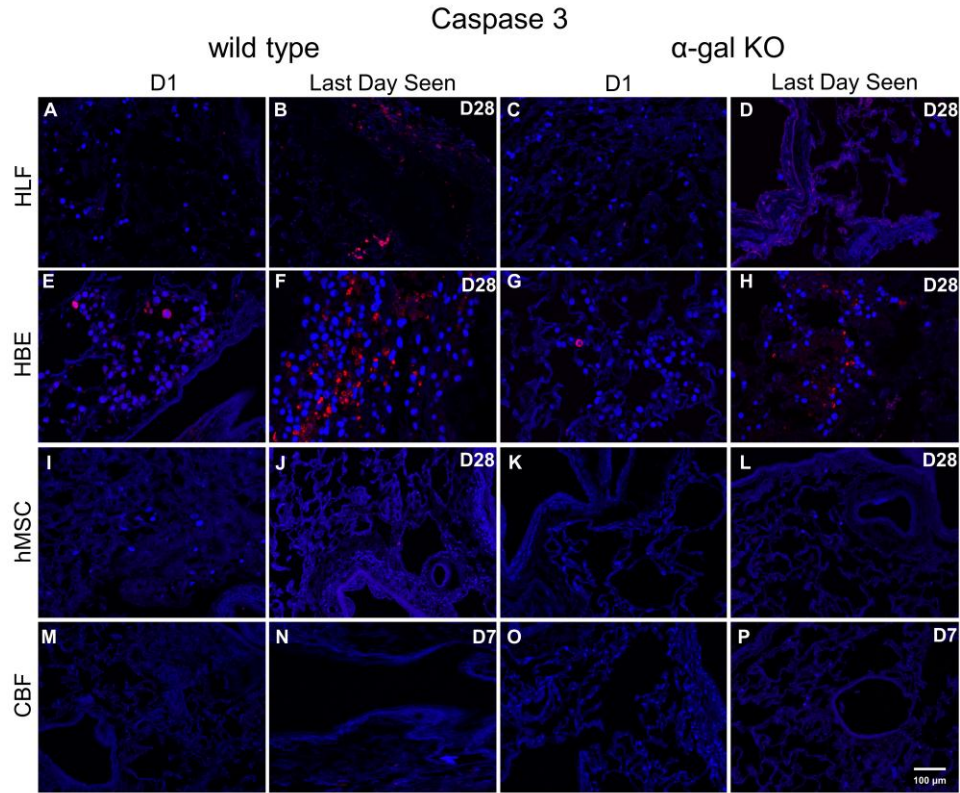
airspaces or vascular spaces unattached to any matrix demonstrated rounding up of cells and nuclear fragmentation, consistent with anoikis or apoptosis.

Figure 7A



Tissue Engineering Part C: Methods  
Comparative study to the use of decellularized alpha-Gal KO pig lungs for xenogeneic lung transplantation (doi: 10.1089/ten.TEC.2016.0109)  
This article has been peer-reviewed and accepted for publication, but has yet to undergo copyediting and proof correction. The final published version may differ from this proof.

Figure 7B



**Figure 7: Cells seeded into wild type vs  $\alpha$ -gal KO pig lungs demonstrate similar patterns of Ki67 and caspase-3 staining. A, B)** Representative photomicrographs one day post-inoculation of each cell type and the last day viable cells were observed are depicted. Original magnification 100X. Ki67 or caspase-3 staining is indicated in red and DAPI nuclear staining in blue. Representative images from 3 wild type and 3  $\alpha$ -gal KO lungs seeded with each cell type are depicted. **C)** Quantitative analysis of randomized images from 3 wild type and 3  $\alpha$ -gal KO lungs seeded with each individual cell type. 4 regions/slide from each seeding and time point were quantified to determine the percentage of ratio of positive stained Ki67 or caspase-3 expressing cells (red staining = Ki67/caspase-3) to total cells (blue staining = DAPI).

**Supplemental Figure 1: Detection of residual anionic detergents in wash effluents during decellularization demonstrated no differences between wild type and  $\alpha$ -gal KO pig lungs.** Depicted is SDC concentration in consecutive DI water washes after incubation of the lungs with the respective decellularization solution. The data from the wild type lungs was already published before as absolute absorption at 630 nm (27) but converted to SDC % concentration and utilized as comparison for the  $\alpha$ -gal KO pig lung effluents.

**Supplemental Figure 2: Isolectin B4 staining in incompletely decellularized wild type pig lungs demonstrates residual  $\alpha$ -galactosylated proteins or protein debris.** Representative image from an incompletely decellularized wild type pig lung demonstrates areas of positive (red) staining (arrow, insert) can be observed in both non-adsorbed and galactose-preadsorbed lectin stainings along with residual DAPI-positive (blue) cell nuclei. Original magnification 200X.

## Supplemental Tables and Figure

### Comparative Decellularization and Recellularization of Wild Type and Alpha 1,3 Galactosyltransferase Knockout Pig Lungs: A Model for *Ex Vivo* Xenogeneic Lung Bioengineering and Transplantation

Joseph Platz<sup>a#</sup>, Nicholas R. Bonenfant<sup>a#</sup>, Franziska E. Uhl<sup>a</sup>, Amy L. Coffey<sup>a</sup>, Tristan McKnight<sup>a</sup>, Charles Parsons,<sup>a</sup> Dino Sokocevic<sup>a,1</sup>, Zachary D. Borg<sup>a</sup>, Ying Wai Lam<sup>b</sup>, Bin Deng<sup>b</sup>, Julia G. Fields<sup>b</sup>, Michael DeSarno<sup>c</sup>, Roberto Loi<sup>d</sup>, Andrew M. Hoffman<sup>e</sup>, John Bianchi<sup>g</sup>, Brian Dacken<sup>h</sup>, Thomas Petersen<sup>i</sup>, Darcy E. Wagner<sup>a,j</sup>, Daniel J. Weiss<sup>a,\*</sup>

**Supplemental Table 1: Details of Decellularization Protocol**

	solution		amount (Liters)		
			via trachea	via pulmonary artery	total
<b>Day one</b>	DI water <b>5x PS</b>	washing	3x 2-3	3x 2-3	12-18
	0.1 % Triton	washing	2-3	2-3	4-6
	0.1 % Triton	filling	2-3	2-3	4-6
<b>Day two</b>	DI water <b>5x PS</b>	washing	3x 2-3	3x 2-3	12-18
	2% SDC	washing	2-3	2-3	4-6
	2% SDC	filling	2-3	2-3	4-6
<b>Day three</b>	DI water <b>1x PS</b>	washing	3x 2-3	3x 2-3	12-18
	1M NaCl	washing	2-3	2-3	4-6
	1M NaCl	filling	2-3	2-3	4-6
	DI water <b>1x PS</b>	washing	3x 2-3	3x 2-3	12-18
	DNase	washing	2-3	2-3	4-6
	DNase	filling	2-3	2-3	4-6
	DI water <b>1x PS</b>	washing	3x 2-3	3x 2-3	12-18
	Peracetic acid	washing	2-3	2-3	4-6
	Peracetic acid	filling	2-3	2-3	4-6
	DI water <b>1x PS</b>	washing	3x 2-3	3x 2-3	12-18
	Storage solution	washing	2x 2-3	2x 2-3	8-12
	Storage solution	filling	2-3	2-3	4-6

PS: penicillin-streptomycin

**Supplementary Table 2.** Spearman rank correlation coefficients comparing mass spectrometry proteomic peptide hits of positively identified proteins in individual samples from decellularized  $\alpha$ -gal KO ( $\alpha$ Gal) and wild type (WT) pig lungs

Variable	aGal_1	aGal_2	aGal_3	aGal_4	aGal_5	aGal_6	aGal_7	aGal_8	aGal_9	aGal_10	WT_1	WT_2	WT_3	WT_4	WT_5	WT_6
<b>aGal_1</b>																
<b>aGal_2</b>	0.85															
<b>aGal_3</b>	0.82	0.80														
<b>aGal_4</b>	0.73	0.77	0.74													
<b>aGal_5</b>	0.81	0.84	0.81	0.75												
<b>aGal_6</b>	0.76	0.77	0.82	0.75	0.79											
<b>aGal_7</b>	0.63	0.73	0.68	0.66	0.66	0.59										
<b>aGal_8</b>	0.67	0.74	0.76	0.63	0.67	0.67	0.86									
<b>aGal_9</b>	0.66	0.74	0.68	0.65	0.68	0.64	0.75	0.75								
<b>aGal_10</b>	0.72	0.81	0.73	0.65	0.70	0.67	0.77	0.79	0.91							
<b>WT_1</b>	0.55	0.60	0.54	0.56	0.52	0.45	0.74	0.71	0.78	0.76						
<b>WT_2</b>	0.44	0.44	0.38	0.54	0.42	0.39	0.49	0.48	0.65	0.60	0.74					
<b>WT_3</b>	0.52	0.55	0.54	0.58	0.51	0.50	0.69	0.67	0.76	0.77	0.85	0.78				
<b>WT_4</b>	0.54	0.55	0.56	0.60	0.51	0.49	0.72	0.69	0.77	0.74	0.86	0.76	0.89			
<b>WT_5</b>	0.48	0.52	0.51	0.56	0.46	0.48	0.65	0.58	0.69	0.68	0.83	0.70	0.85	0.85		
<b>WT_6</b>	0.56	0.61	0.66	0.51	0.54	0.54	0.72	0.74	0.66	0.63	0.61	0.30	0.58	0.64	0.62	

**Supplementary Table 3.** Spearman rank p-values comparing mass spectrometry proteomic peptide hits of positively identified proteins in individual samples from decellularized  $\alpha$ -Gal KO ( $\alpha$ Gal) and wild type (WT) pig lungs

Variable	aGal_1	aGal_2	aGal_3	aGal_4	aGal_5	aGal_6	aGal_7	aGal_8	aGal_9	aGal_10	WT_1	WT_2	WT_3	WT_4	WT_5	WT_6
<b>aGal_1</b>																
<b>aGal_2</b>	< 0.0001															
<b>aGal_3</b>	< 0.0001	< 0.0001														
<b>aGal_4</b>	< 0.0001	< 0.0001	< 0.0001													
<b>aGal_5</b>	< 0.0001	< 0.0001	< 0.0001	< 0.0001												
<b>aGal_6</b>	< 0.0001	< 0.0001	< 0.0001	< 0.0001	< 0.0001											
<b>aGal_7</b>	< 0.0001	< 0.0001	< 0.0001	< 0.0001	< 0.0001	< 0.0001										
<b>aGal_8</b>	< 0.0001	< 0.0001	< 0.0001	< 0.0001	< 0.0001	< 0.0001	< 0.0001									
<b>aGal_9</b>	< 0.0001	< 0.0001	< 0.0001	< 0.0001	< 0.0001	< 0.0001	< 0.0001	< 0.0001								
<b>aGal_10</b>	< 0.0001	< 0.0001	< 0.0001	< 0.0001	< 0.0001	< 0.0001	< 0.0001	< 0.0001	< 0.0001							
<b>WT_1</b>	< 0.0001	< 0.0001	< 0.0001	< 0.0001	< 0.0001	< 0.0001	< 0.0001	< 0.0001	< 0.0001	< 0.0001						
<b>WT_2</b>	< 0.0001	< 0.0001	< 0.0001	< 0.0001	< 0.0001	< 0.0001	< 0.0001	< 0.0001	< 0.0001	< 0.0001	< 0.0001					
<b>WT_3</b>	< 0.0001	< 0.0001	< 0.0001	< 0.0001	< 0.0001	< 0.0001	< 0.0001	< 0.0001	< 0.0001	< 0.0001	< 0.0001	< 0.0001				
<b>WT_4</b>	< 0.0001	< 0.0001	< 0.0001	< 0.0001	< 0.0001	< 0.0001	< 0.0001	< 0.0001	< 0.0001	< 0.0001	< 0.0001	< 0.0001	< 0.0001			
<b>WT_5</b>	< 0.0001	< 0.0001	< 0.0001	< 0.0001	< 0.0001	< 0.0001	< 0.0001	< 0.0001	< 0.0001	< 0.0001	< 0.0001	< 0.0001	< 0.0001	< 0.0001		
<b>WT_6</b>	< 0.0001	< 0.0001	< 0.0001	< 0.0001	< 0.0001	< 0.0001	< 0.0001	< 0.0001	< 0.0001	< 0.0001	< 0.0001	0.0011	< 0.0001	< 0.0001	< 0.0001	

**Supplemental Table 4 – Total spectral counts for positively identified proteins in acellular  $\alpha$ -gal KO and wildtype (WT) lungs**

Gene Name	Accession No.	Alpha-gal KO										WT (by Sample)											
		1	2	3	4	5	6	7	8	9	10	1A	1B	2A	2B	3A	3B	4A	4B	5A	5B	6A	6B
<b>Cytoplasmic</b>																							
CBR2	CBR2_PIG	10	6	4	3	9	8	11	19	4	13	11	14	39	40	18	15	18	23	20	19	5	14
DPYSL2	I3LJE2_PIG	8	7	7	4	3	3	3	5	4	2	0	3	4	3	0	0	0	6	0	0	0	0
EEF1A	Q0PY11_PIG	0	2	0	4	2	1	2	0	4	0	5	4	9	9	0	0	4	3	5	0	7	0
EEF2	I3LII3_PIG	6	6	7	4	7	6	2	3	0	1	0	0	7	4	0	0	0	0	0	0	0	0
HSPB1	HSPB1_PIG	0	2	3	8	5	1	8	0	4	3	5	7	9	6	4	0	4	6	7	4	0	0
HSPG2	F1SU03_PIG	3	3	2	4	1	0	4	0	3	1	0	0	0	0	0	0	5	0	6	5	4	
Ssc.41914	F1STM4_PIG	0	0	0	0	2	0	0	0	0	0	0	0	0	0	0	0	0	0	0	0	0	0
<b>Cytoskeletal</b>																							
ACTA2	C7AI81_PIG	8	10	9	11	14	12	15	17	20	20	20	30	38	30	25	27	22	20	26	19	22	7
ACTB	ACTB_PIG	17	13	12	16	13	10	19	18	22	22	34	44	52	43	35	39	35	30	29	24	16	15
ACTC1	B6VNT8_PIG	8	11	10	12	14	12	16	19	21	23	22	30	38	31	25	27	22	20	26	19	22	7
CCT6A	F1RIU3_PIG	4	8	3	7	6	4	0	0	0	0	0	0	0	0	0	0	0	0	0	0	0	0
DES	DESM_PIG	6	8	6	7	11	8	7	4	17	13	6	3	10	10	5	0	3	0	5	0	4	0
EZR	F1SB42_PIG	3	0	0	1	0	0	3	0	0	0	0	0	0	0	0	0	0	0	0	0	0	0
FLNC	F1SMN5_PIG	4	3	0	3	4	0	0	0	1	2	0	0	0	0	0	0	0	0	0	0	0	0
HBA	HBA_PIG	4	4	6	4	4	3	5	9	17	11	28	29	26	22	23	22	28	26	40	43	11	20
	I3LJ44_PIG	8	8	8	4	8	6	11	10	14	15	10	12	9	10	14	15	12	14	11	13	5	11
KRT19	F1S0J8_PIG	1	0	0	1	2	0	2	4	5	0	0	0	4	0	0	0	0	0	0	0	7	4
LOC100511457_1	I3LV99_PIG	2	5	0	3	3	3	1	0	5	4	0	0	0	0	0	0	0	0	0	0	0	0
LOC100511457_2	I3LIE3_PIG	2	5	3	4	4	4	1	0	5	4	0	0	0	0	0	0	0	0	0	0	0	0
LOC100517284	F1RI39_PIG	3	3	3	3	2	0	0	0	2	0	4	0	5	4	0	0	0	0	0	0	5	2
LOC100620928	F1S6M7_PIG	16	10	11	8	11	16	7	11	15	15	15	19	20	16	11	10	22	17	13	11	13	10
LOC100621514	I3LDR2_PIG	4	8	6	9	5	9	7	8	5	4	5	4	0	0	0	6	0	9	4	13	9	
LOC100621981	I3L5B3_PIG	26	29	27	27	26	29	35	31	37	35	22	19	16	16	25	31	26	26	15	17	11	28
MACF1	F1SV22_PIG	3	4	3	2	6	0	4	3	0	2	0	3	0	0	0	4	5	0	0	0	0	6

MSN	F1RTN3_PIG	4	2	0	2	2	0	3	0	0	2	0	6	0	4	0	0	0	0	0	0	0	
MYH10	F1SSA6_PIG	34	36	34	34	34	45	38	37	38	37	24	21	16	16	27	34	29	28	15	17	18	32
MYH11_1	F1SK10_PIG	12	6	15	13	10	12	8	8	7	10	10	11	0	0	5	5	6	6	0	6	18	5
MYH11_2	MYH11_PIG	4	3	7	3	5	4	2	5	0	0	0	0	0	0	0	0	0	0	0	0	9	0
MYH9	F1SKJ1_PIG	45	46	34	48	44	53	50	34	58	75	61	59	77	75	85	104	88	87	99	110	53	49
MYL6	MYL6_PIG	3	2	3	3	1	2	0	3	5	5	13	12	8	7	5	0	4	3	4	4	0	0
MYO1C	I3LIL4_PIG	6	6	8	8	9	8	7	9	4	4	9	4	3	4	4	3	7	8	9	6	0	2
NUMA1	F1SUX4_PIG	1	0	0	0	2	1	4	2	4	2	0	0	0	0	0	0	0	0	0	0	0	2
TLN1	F1SFZ8_PIG	6	6	5	9	9	2	20	12	5	5	15	14	18	25	16	19	18	20	16	17	0	9
TPM3	Q6QA25_PIG	1	4	0	0	0	0	4	3	0	2	3	0	0	0	0	0	0	0	0	0	0	0
TUBA1B	F2Z5T5_PIG	19	17	20	18	18	29	11	12	8	5	13	17	9	10	9	9	15	12	16	17	18	11
TUBA4A	F2Z5S8_PIG	8	11	10	12	7	12	11	12	5	4	8	7	5	6	5	5	12	5	11	4	13	12
TUBB	TBB5_PIG	23	21	24	21	21	27	18	22	25	28	28	32	33	40	23	20	38	31	29	26	15	15
TUBB1	A5GFX6_PIG	4	4	0	2	4	2	2	0	4	4	5	6	0	0	0	3	6	0	0	4	7	5
TUBB2B	F2Z5B2_PIG	19	15	17	12	14	24	14	17	20	22	18	22	20	25	11	10	28	17	15	13	13	10
TUBB4A	F2Z5K5_PIG	20	12	15	14	13	17	8	10	15	16	13	18	18	18	11	9	19	14	11	9	11	10
TUBB4B	F2Z571_PIG	21	15	18	17	16	23	15	18	22	25	19	25	26	27	14	10	31	20	16	11	13	10
TUBB6	I3LBV1_PIG	6	5	3	2	5	5	2	3	7	6	6	8	5	4	0	3	6	5	4	4	7	5
	I3LCX2_PIG	8	8	13	7	9	6	13	12	10	14	9	6	3	0	11	10	9	12	9	4	9	10
	F1RJU6_PIG	0	0	0	0	0	0	0	0	3	0	0	0	0	0	0	0	0	0	0	0	0	0
	I3LIQ9_PIG	4	11	4	10	4	6	10	11	7	12	6	10	10	7	16	9	12	9	16	13	9	10
VCL	VINC_PIG	0	0	0	0	0	0	3	3	0	0	4	4	7	6	0	0	4	5	0	0	0	0
VIM	VIME_PIG	11	7	9	5	11	9	2	3	22	7	11	17	21	27	4	3	7	8	9	11	4	4
<b>Cytosolic</b>																							
YWHAZ	F2Z558_PIG	2	0	2	1	3	4	0	0	0	0	0	0	0	0	0	0	0	0	0	0	0	0
<b>ECM</b>																							
COL14A1	F1S285_PIG	4	4	3	4	4	5	2	4	2	0	0	6	3	3	0	5	0	0	0	0	4	6
COL1A1	F1RT61_PIG	0	2	2	0	2	3	0	3	4	5	0	0	5	3	5	0	0	0	0	0	0	0
COL1A2	F1SFA7_PIG	2	1	5	3	2	3	4	11	8	10	11	11	5	6	14	10	15	8	15	11	20	10
COL6A1	I3LS72_PIG	5	6	3	2	5	3	6	4	9	8	0	0	0	0	0	5	0	6	0	0	5	10

COL6A3	I3LUR7_PIG	100	85	87	75	96	83	75	92	96	84	78	86	65	73	147	136	109	103	122	121	116	116	
COL6A5	F1RS99_PIG	10	7	4	4	10	7	8	19	3	4	5	4	0	0	0	0	0	0	0	0	0	0	7
EMILIN1	F1SDQ5_PIG	2	2	3	0	3	0	0	4	0	0	0	0	0	3	4	0	4	3	4	4	5	2	
FBN1_1	FBN1_PIG	8	18	32	15	18	18	13	25	5	8	3	0	0	0	0	0	4	5	0	0	60	56	
FBN1_2	F1SN67_PIG	8	15	28	14	16	18	11	22	4	7	0	0	0	0	0	0	3	3	0	0	56	48	
FN1	F1SS24_PIG	15	14	10	8	7	2	17	5	12	17	19	15	9	9	7	10	10	16	15	13	20	16	
I3LAA4	I3LAA4_PIG	3	0	2	1	2	3	7	8	4	0	0	4	0	0	0	0	6	6	0	0	5	11	
I3LQ84	I3LQ84_PIG	15	15	20	23	17	21	16	19	18	20	17	18	14	15	30	31	12	11	9	11	33	16	
LAMA4	F1RZM4_PIG	2	2	3	0	2	2	1	2	0	3	0	0	0	0	0	0	0	0	4	0	0	0	
LAMB1	F1SAE9_PIG	3	2	3	2	3	3	3	0	0	0	0	0	0	0	0	0	0	0	4	0	13	11	
LAMB2	F1SPT5_PIG	3	6	13	10	7	11	7	8	10	11	5	7	0	3	12	14	3	12	7	11	16	14	
LAMC1	F1S663_PIG	9	7	13	9	10	12	6	8	7	5	0	0	3	0	4	7	7	9	5	4	16	25	
LOC100739576	I3L9T6_PIG	3	2	8	4	4	3	2	4	3	2	0	0	0	0	0	0	0	0	0	0	0	9	
POSTN	I3LDM1_PIG	3	6	7	6	5	4	7	8	2	4	4	7	0	0	7	5	0	0	4	0	9	7	
TGFBI_1	BGH3_PIG	24	20	13	10	19	20	17	11	8	9	4	8	3	6	14	7	7	0	11	11	0	6	
TGFBI_2	F1RHA7_PIG	11	11	7	4	9	11	12	5	4	5	5	10	4	7	12	5	4	0	0	4	0	6	
TGM2	F1SDX6_PIG	8	15	9	13	12	13	18	12	16	19	24	24	20	21	23	14	19	17	13	22	9	6	
TNC_2	F1SMI5_PIG	4	5	3	2	5	3	0	0	3	4	0	0	0	0	0	0	0	0	0	0	0	0	
TNC_1	TENA_PIG	8	7	3	2	7	5	0	0	4	4	0	0	0	0	0	0	0	0	0	0	0	6	
<b>Membrane</b>																								
ANXA1	F1SJB5_PIG	5	3	3	2	6	0	0	0	2	2	4	4	4	3	0	0	4	0	0	0	0	0	
ANXA2	ANXA2_PIG	3	6	1	10	6	0	4	8	4	2	4	3	10	9	0	0	0	0	0	0	4	0	
ATP5A1	ATPA_PIG	0	1	2	7	5	6	3	3	2	0	0	0	0	3	0	0	0	0	0	0	0	0	
ATP5B	F1SLA0_PIG	5	7	2	7	3	9	4	4	3	8	0	0	8	9	0	0	0	0	0	0	0	0	
CLTC	F6PV15_PIG	5	6	4	7	4	8	0	0	0	0	0	0	0	0	0	0	0	0	0	0	0	0	
EHD2	I3LD72_PIG	8	4	4	6	8	2	2	3	3	4	4	4	4	3	0	0	0	0	0	9	0	0	
ENPP6	ENPP6_PIG	3	3	2	0	2	2	0	5	0	3	0	0	0	0	0	0	0	0	0	0	0	0	
IQGAP1_1	I3LDA8_PIG	3	0	4	4	0	3	4	4	0	0	3	0	5	0	0	3	3	3	0	0	0	0	
IQGAP1_2	F1RMJ4_PIG	0	0	3	2	0	0	0	0	0	0	0	0	0	0	0	0	0	0	0	0	0	0	
LOC100049693	F1RR78_PIG	7	8	3	6	13	5	7	7	8	4	15	8	12	13	7	7	6	9	5	19	0	0	

PLG	F1SB81_PIG	0	4	0	0	2	0	4	7	2	2	4	8	0	0	0	0	5	0	0	0	4	
VDAC2	VDAC2_PIG	2	2	2	4	0	0	3	3	2	2	4	4	3	0	4	7	3	6	5	6	7	5
<b><u>Nuclear</u></b>																							
DHX9	I3LHZ6_PIG	4	3	0	4	3	1	0	0	0	2	0	0	0	0	0	0	0	0	0	0	0	
F1SSL5	F1SSL5_PIG	0	0	2	0	0	3	0	0	0	0	0	0	4	3	0	0	0	0	0	0	0	
H2AFV	F2Z5P1_PIG	0	0	0	3	0	0	2	0	0	0	5	0	4	4	0	3	3	5	0	0	0	
H2AFX	I3L7T6_PIG	0	0	0	3	0	0	3	0	0	0	8	0	8	7	7	7	4	6	4	4	0	
H3F3A	H33_PIG	0	3	0	0	3	0	4	4	4	3	10	4	5	6	7	7	7	8	4	6	0	
H4	H4_PIG	1	2	2	4	4	7	6	5	4	4	11	10	9	7	18	20	21	16	7	9	13	
HIST1H2BD	F2Z584_PIG	10	9	10	7	9	10	4	6	12	14	9	8	22	27	11	17	13	12	11	0	0	
HIST1H2BN	F2Z579_PIG	10	9	10	7	9	10	4	6	12	14	9	8	22	27	11	17	13	12	11	0	0	
HIST2H2AA4	F2Z5L2_PIG	0	4	0	6	3	3	4	4	5	7	13	7	23	22	16	14	15	16	11	13	0	
HIST2H2AB	F2Z5L6_PIG	0	0	0	2	2	0	0	0	0	0	4	0	4	3	5	3	3	3	0	0	0	
HNRNPK	I3LQS0_PIG	11	10	10	9	8	5	5	5	2	4	6	7	7	10	12	10	9	9	11	11	11	
HNRNPU	F1S8L9_PIG	1	0	2	1	4	3	3	0	0	0	0	0	0	0	0	0	0	0	4	0	0	
LMNA_1	LMNA_PIG	6	3	3	5	4	0	8	8	7	7	6	7	8	9	7	7	6	3	0	0	4	
LMNA_2	F1RLQ2_PIG	5	3	3	4	4	0	8	8	5	7	6	7	8	9	7	7	6	3	0	0	4	
LOC100152878	F1RTQ5_PIG	3	2	2	3	2	3	1	3	1	2	0	0	7	3	0	0	3	0	0	0	0	
LOC100155734	F2Z587_PIG	0	4	0	6	3	0	3	3	5	3	10	6	16	15	11	10	10	11	9	9	0	
LOC100157763	F1RPL3_PIG	0	0	0	6	0	3	3	4	5	7	13	7	22	22	12	10	10	11	9	9	0	
LOC100524253	F2Z5L0_PIG	10	8	10	6	10	10	4	7	12	13	0	0	18	22	9	12	12	0	0	0	0	
LOC100525821	F2Z576_PIG	0	3	0	0	3	0	3	3	4	3	9	3	5	4	11	5	7	8	4	6	9	
LOC100622412	F2Z5K9_PIG	0	3	0	0	3	0	6	3	4	3	13	4	8	6	9	5	6	9	5	9	0	
MYBBP1A	F1RGP1_PIG	0	0	2	0	0	3	0	0	0	0	0	0	0	0	0	0	6	0	9	0	0	
<b><u>Secreted</u></b>																							
C3_1	CO3_PIG	4	4	6	0	3	2	8	5	2	5	11	10	0	0	5	3	4	0	5	4	4	
C3_2	F1SBS4_PIG	0	0	0	0	0	0	0	0	0	0	0	3	0	0	0	0	0	0	0	0	0	
FGA_1	F1RX36_PIG	6	15	9	4	6	3	18	23	18	17	9	14	4	4	7	5	7	8	5	0	9	
FGA_2	I3LQR9_PIG	0	13	9	0	6	3	17	23	14	14	0	10	0	0	0	0	0	0	0	0	0	
FGB	F1RX37_PIG	14	15	12	7	9	6	19	26	22	22	19	21	0	0	5	7	7	9	4	4	13	

HBB_1	F1RII7_PIG	9	9	5	4	0	5	10	11	20	23	25	32	21	25	14	22	19	22	40	50	24	21
HBB_2	HBB_PIG	8	7	4	4	0	3	8	11	19	20	22	28	10	16	14	19	19	19	35	45	16	16
HBE1	F1RII6_PIG	0	0	0	0	0	0	3	3	0	0	0	0	0	0	0	0	0	0	5	0	0	0
LOC100627396	F1RX35_PIG	16	15	10	7	12	7	16	32	13	17	19	17	0	0	9	12	10	12	9	4	22	11
VWF	VWF_PIG	4	7	0	4	2	3	3	0	0	0	0	0	0	0	0	0	0	0	0	0	0	0
<u>Unknown</u>																							
I3LP72	I3LP72_PIG	0	0	0	0	0	0	2	0	0	0	0	0	0	0	0	0	0	0	0	6	0	6

**Supplementary Table 5.** Mass spectrometry proteomic assessment of acellular alpha-gal and wild type porcine lungs by cellular location. FDR-corrected exact p-values less than 0.05 are considered statistically significant and are bolded. Shaded boxes indicates unique peptide count median was significantly higher in acellular  $\alpha$ -gal KO porcine lungs than acellular wild type (WT) porcine lungs

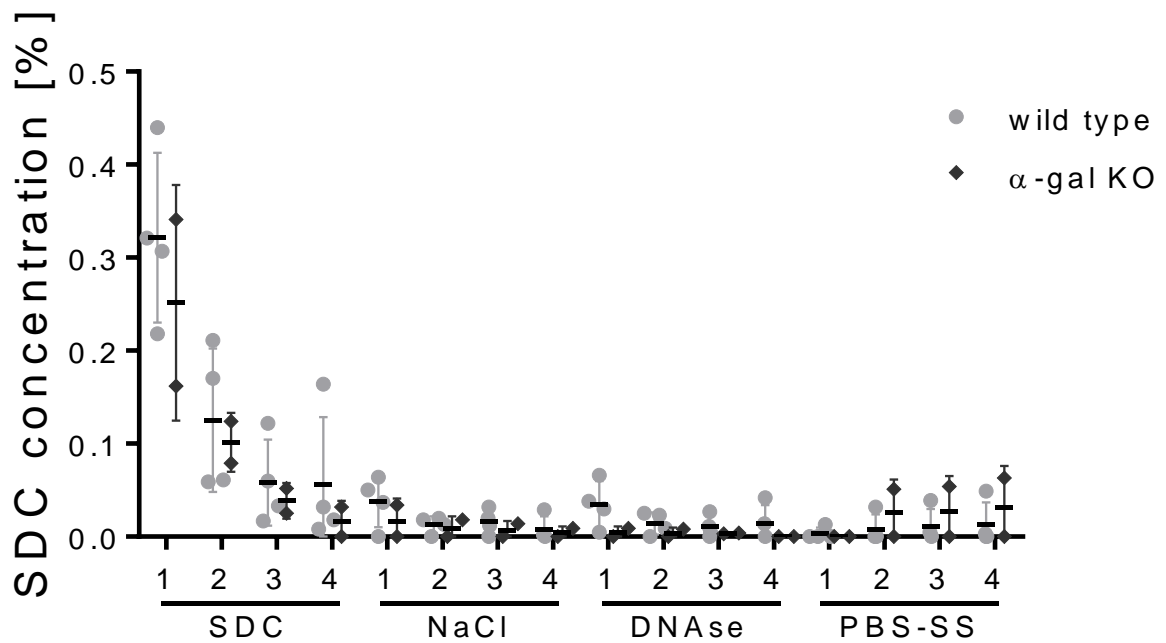
<b>Alpha-gal vs Normal pig lung proteomic comparisons</b>			
<b>Gene name</b>	<b>Accession #</b>	<b>Exact p-value</b>	<b>FDR-corrected exact p-value</b>
<b>Cytoplasmic</b>			
<b>CBR2</b>	<b>CBR2</b>	0.0047	<b>0.030</b>
<b>DPYSL2</b>	<b>I3LJE2</b>	0.0082	<b>0.039</b>
EEF2	I3LII3	0.0272	0.089
EEF1A	Q0PY11	0.0326	0.099
HSPB1	HSPB1	0.4961	0.641
HSPG2	F1SU03	0.6139	0.728
Ssc_41914	F1STM4	1.0000	1.009
<b>Cytoskeletal</b>			
<b>MYH10</b>	<b>F1SSA6</b>	0.0001	<b>0.014</b>
<b>HBA</b>	<b>HBA</b>	0.0002	<b>0.007</b>
<b>ACTB</b>	<b>ACTB</b>	0.0010	<b>0.019</b>
<b>ACTA2</b>	<b>C7AI81</b>	0.0015	<b>0.019</b>
<b>MYH9</b>	<b>F1SKJ1</b>	0.0019	<b>0.020</b>
<b>LOC100621981</b>	<b>I3L5B3</b>	0.0020	<b>0.019</b>
<b>LOC100511457_2</b>	<b>I3LIE3</b>	0.0020	<b>0.018</b>
<b>ACTC1</b>	<b>B6VNT8</b>	0.0062	<b>0.033</b>
<b>LOC100511457_1</b>	<b>I3LV99</b>	0.0082	<b>0.038</b>
TLN1	F1SFZ8	0.0204	0.071
DES	DESM	0.0282	0.090
NUMA1	F1SUX4	0.0331	0.098
MYH11_2	MYH11	0.0382	0.110
CCT6A	F1RIU3	0.0451	0.121
MYH11_1	F1SKIO	0.0478	0.125
FLNC	F1SMN5	0.0495	0.126
VCL	VINC	0.1071	0.216
TPM3	Q6QA25	0.1140	0.226

I3LIQ9	I3LIQ9	0.1154	0.221
MYL6	MYL6	0.1266	0.239
TUBB	TBB5	0.1344	0.241
MYO1C	I3LIL4	0.1356	0.240
I3LJ44	I3LJ44	0.1561	0.272
LOC100620928	F1S6M7	0.1617	0.278
LOC100621514	I3LDR2	0.1658	0.280
I3LCX2	I3LCX2	0.1883	0.314
MACF1	F1SV22	0.2265	0.372
EZR	F1SB42	0.3393	0.494
TUBA4A	F2Z5S8	0.3610	0.506
MSN	F1RTN3	0.3679	0.510
TUBA1B	F2Z5T5	0.4106	0.549
VIM	VIME	0.5995	0.718
TUBB6	I3LBV1	0.6379	0.749
TUBB1	A5GFX6	0.7365	0.856
TUBB4A	F2Z5K5	0.7474	0.859
KRT19	F1S0J8	0.7490	0.853
TUBB2B	F2Z5B2	0.7793	0.879
LOC100517284	F1RI39	0.8156	0.911
TUBB4B	F2Z571	0.8638	0.920
F1RJU6	F1RJU6	1.0000	1.018
YWHAZ	F2Z558	0.0865	0.188
<b>ECM</b>			
<b>TGFBI_1</b>	<b>BGH3</b>	0.0050	<b>0.030</b>
<b>COL1A2</b>	<b>F1SFA7</b>	0.0051	<b>0.029</b>
<b>TNC_2</b>	<b>F1SMI5</b>	0.0052	<b>0.029</b>
<b>COL6A5</b>	<b>F1RS99</b>	0.0062	<b>0.031</b>
<b>LOC100739576</b>	<b>I3L9T6</b>	0.0102	<b>0.044</b>
LAMA4	F1RZM4	0.0145	0.059
TNC_1	TENA	0.0175	0.069
COL6A1	I3LS72	0.0403	0.110
COL6A3	I3LUR7	0.0528	0.127
TGFBI_2	F1RHA7	0.0628	0.142
TGM2	F1SDX6	0.0912	0.194
EMILIN1	F1SDQ5	0.1324	0.246
COL14A1	F1S285	0.2276	0.369
POSTN	I3LDM1	0.2576	0.406
FN1	F1SS24	0.3209	0.486
COL1A1	F1RT61	0.3584	0.509
LAMC1	F1S663	0.4609	0.602

FBN1_2	F1SN67	0.5217	0.659
FBN1_1	FBN1	0.5456	0.682
I3LQ84	I3LQ84	0.8370	0.917
I3LAA4	I3LAA4	0.8534	0.917
LAMB1	F1SAE9	0.8934	0.934
LAMB2	F1SPT5	0.9647	0.990
<b>Membrane</b>			
<b>VDAC2</b>	<b>VDAC2</b>	0.0085	<b>0.038</b>
ATP5A1	ATPA	0.0192	0.071
ENPP6	ENPP6	0.0202	0.073
ATP5B	F1SLA0	0.0214	0.072
CLTC	F6PV15	0.0395	0.111
EHD2	I3LD72	0.0584	0.137
ANXA2	ANXA2	0.2798	0.435
LOC100049693	F1RR78	0.3529	0.507
IQGAP1_1	I3LDA8	0.4027	0.545
ANXA1	F1SJB5	0.4188	0.554
IQGAP1_2	F1RMJ4	0.5000	0.639
PLG	F1SB81	0.8330	0.921
<b>Nuclear</b>			
<b>LOC100525821</b>	<b>F2Z576</b>	0.0001	<b>0.005</b>
<b>H4</b>	<b>H4</b>	0.0001	<b>0.007</b>
<b>LOC100622412</b>	<b>F2Z5K9</b>	0.0004	<b>0.009</b>
<b>HIST2H2AA4</b>	<b>F2Z5L2</b>	0.0015	<b>0.022</b>
<b>H2AFX</b>	<b>I3L7T6</b>	0.0017	<b>0.020</b>
<b>H3F3A</b>	<b>H33</b>	0.0027	<b>0.023</b>
<b>LOC100155734</b>	<b>F2Z587</b>	0.0037	<b>0.029</b>
<b>LOC100157763</b>	<b>F1RPL3</b>	0.0045	<b>0.030</b>
HIST2H2AB	F2Z5L6	0.0176	0.067
DHX9	I3LHZ6	0.0507	0.124
H2AFV	F2Z5P1	0.0619	0.142
HNRNPK	I3LQS0	0.0773	0.171
HNRNPU	F1S8L9	0.1058	0.217
LOC100152878	F1RTQ5	0.1141	0.222
MYBBP1A	F1RGP1	0.2335	0.373
LOC100524253	F2Z5L0	0.3252	0.486
HIST1H2BN	F2Z579	0.5987	0.725
HIST1H2BD	F2Z584	0.5987	0.732
F1SSL5	F1SSL5	0.8393	0.911
LMNA_1	LMNA	0.8841	0.933
LMNA_2	F1RLQ2	0.8965	0.929

<u>Secreted</u>			
<b>HBB_1</b>	<b>F1RII7</b>	0.0011	<b>0.018</b>
<b>HBB_2</b>	<b>HBB</b>	0.0044	<b>0.031</b>
FGA_2	I3LQR9	0.0303	0.094
VWF	VWF	0.0495	0.124
FGB	F1RX37	0.0957	0.200
FGA_1	F1RX36	0.1340	0.245
LOC100627396	F1RX35	0.3084	0.473
C3_2	F1SBS4	0.3750	0.513
C3_1	CO3	0.5868	0.726
HBE1	F1RII6	1.0000	1.000
<u>Unknown</u>			
I3LP72	I3LP72	0.3393	0.500

**Supplemental Figure 1: Anionic detergent detection of effluents during decellularization of wild type and  $\alpha$ -gal KO pig lungs revealed no significant differences.** SDC concentration consecutive DI water washes after incubation of the lungs with the respective solution. The data from the wild type lungs was already published before as absolute absorption at 630 nm (27) but converted to SDC % concentration.



**Supplemental Figure 2: Isolectin B4 staining in incompletely decellularized wild type pig lungs demonstrates residual  $\alpha$ -galactosylated proteins or protein debris.** Representative image from an incompletely decellularized wild type pig lung demonstrates areas of positive (red) staining (arrow, insert) can be observed in both non-adsorbed and galactose-preadsorbed lectin stainings along with residual DAPI-positive (blue) cell nuclei. Original magnification 200X.

